Airway epithelial responses to rhinovirus, coronavirus and cigarette smoke

Wang, Y.

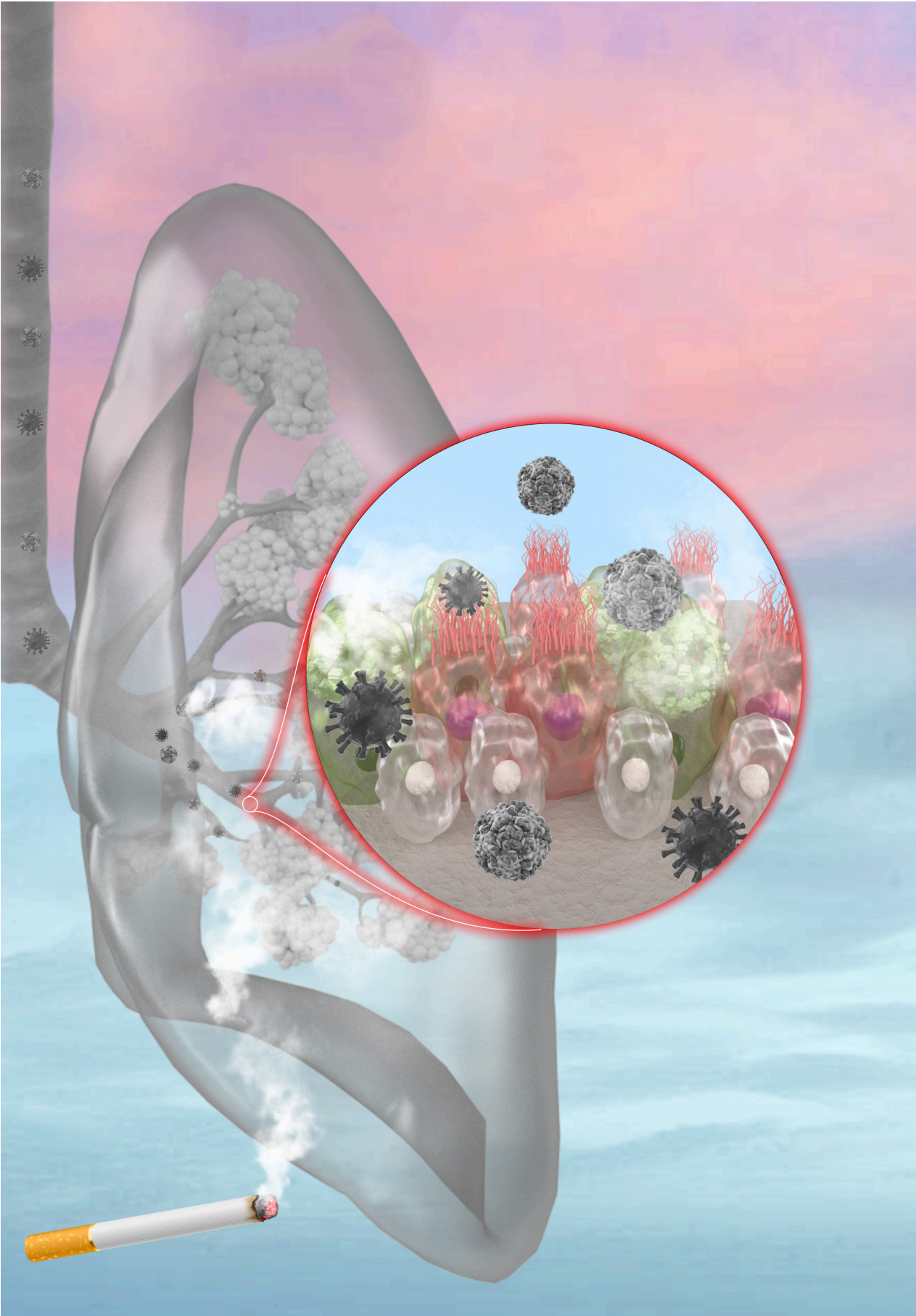

Chapter 2

Dysregulated mitochondrial metabolism upon cigarette smoke exposure in various human bronchial epithelial cell models

Ying Wang[2]*, Christy B.M. Tulen, [1]*, Daan Beentjes[2], Phyllis J.J. Jessen[1], Dennis K. Ninaber[2], Niki L. Reynaert[3,4], Frederik-Jan van Schooten[1], Antoon Opperhuizen[1,5], Pieter S. Hiemstra[2], Alexander H.V. Remels[1]

[1]Department of Pharmacology and Toxicology, School of Nutrition and Translational Research in Metabolism (NUTRIM), Maastricht University Medical Center+, Maastricht, the Netherlands

[2]Department of Pulmonology, Leiden University Medical Center, Leiden, the Netherlands.

[3]Department of Respiratory Medicine, School of Nutrition and Translational Research in Metabolism (NUTRIM), Maastricht University Medical Center+, Maastricht, the Netherlands

[4]Primary Lung Culture Facility (PLUC), Maastricht University Medical Center+, Maastricht, the Netherlands

[5]Netherlands Food and Consumer Product Safety Authority (NVWA), Utrecht, the Netherlands

*Authors contributed equally

Dis Model Mech. 2022 Mar 1;15(3):dmm049247.

Abstract

Exposure to cigarette smoke (CS) is the primary risk factor for developing chronic obstructive pulmonary disease. The impact of CS exposure on the molecular mechanisms involved in mitochondrial quality control in airway epithelial cells is incompletely understood. Undifferentiated or differentiated primary bronchial epithelial cells were acutely/chronically exposed to whole CS (WCS) or CS extract (CSE) in submerged or air–liquid interface conditions. Abundance of key regulators controlling mitochondrial biogenesis, mitophagy and mitochondrial dynamics was assessed. Acute exposure to WCS or CSE increased the abundance of components of autophagy and receptor-mediated mitophagy in all models. Although mitochondrial content and dynamics appeared to be unaltered in response to CS, changes in both the molecular control of mitochondrial biogenesis and a shift toward an increased glycolytic metabolism were observed in particular in differentiated cultures. These alterations persisted, at least in part, after chronic exposure to WCS during differentiation and upon subsequent discontinuation of WCS exposure. In conclusion, smoke exposure alters the regulation of mitochondrial metabolism in airway epithelial cells, but observed alterations may differ between various culture models used.

Introduction

Exposure to cigarette smoke (CS) is the most important risk factor for developing Chronic Obstructive Pulmonary Disease (COPD), a leading cause of mortality and burden of disease worldwide (1, 2). However, whereas much has been learnt about the role of oxidative stress and CS-induced inflammation, our insight into the molecular mechanisms driving smoke-induced COPD pathogenesis still has various knowledge-gaps, including those related to mitochondrial function.

Recent studies have suggested a crucial role for mitochondrial dysfunction in the pathogenesis of smoking-related lung diseases such as COPD (3-8). Indeed, a variety of studies have identified abnormal mitochondrial morphology, e.g., swelling and fragmentation, in airway epithelial cells of COPD patients which was recapitulated in various *in vivo* and *in vitro* experimental exposure models with CS or CS extract (CSE) respectively (3, 9-17). Moreover, in mice, amelioration of CS-induced mitochondrial dysfunction alleviated COPD-associated pathological features (3).

Mitochondrial function and content are regulated by a series of crucial cellular quality control processes, including mitochondrial biogenesis and mitophagy. Mitochondrial biogenesis is essentially regulated via the Peroxisome Proliferator-Activated Receptor Gamma, Coactivator 1 (PPARGC1) signaling network which includes a myriad of transcription factors and transcriptional co-activators (18-20) that cooperatively drive the genesis of new organelles. On the other hand, defective/damaged mitochondria can be degraded by selective autophagy, i.e., mitophagy, which is modulated by two specific pathways (21): *i.* receptor-mediated mitophagy, initiated by mitochondrial receptors, such as BCL2/Adenovirus E1B 19 kDa Protein-Interacting Protein 3 (BNIP3), BNIP3-Like (BNIP3L), and FUN14 Domain Containing 1 (FUNDC1); and *ii.* ubiquitin-mediated mitophagy, triggered by a loss of mitochondrial membrane potential, accumulation of PTEN Induced Kinase 1 (PINK1) and recruitment of Parkin RBR E3 Ubiquitin Protein Ligase (PRKN) in the outer mitochondrial membrane. Evidently, both mitophagy pathways require general autophagy proteins, such as GABA Type A Receptor Associated Protein Like 1 (GABARAPL1), Microtubule-Associated Protein 1B Light Chain 3 (MAP1LC3) Alpha and Beta, and Sequestosome 1 (SQSTM1), to facilitate formation of the autophagosomal membrane around the mitochondrion (22).

Autophagy has been suggested to be critically involved in COPD pathogenesis (23). Previous research indicated that markers of autophagy and mitophagy are induced in lung tissue of COPD patients (9, 24-26). This was confirmed in various models of CS(E) exposure of (human) airway epithelial cells, however most studies deployed cell lines or submerged undifferentiated cultures of primary human airway epithelial cells (9, 11, 16, 24-32), which are not an accurate representation of the complex *in vivo* cellular architecture of the human airway epithelium.

Since epithelial cells that line the respiratory tract are the first cells to be exposed to inhaled toxicants, the relevance of studying the impact of exposure to CS on mitochondrial function and content in airway epithelial cells is obvious (33). However, the epithelial lining of the airways consists of several distinct cell types not all of which are included in most studied cell lines or submerged culture models. Studying the variety of cell types is essential because individual cell types differ in number and intracellular organization of mitochondria that may be related to their function and corresponding energy demand (6). Therefore, a differentiated pseudostratified layer of primary airway epithelial cells including ciliated-, club- and goblet cells, is needed to study these processes in culture models (34). However, previous literature used cell lines or submerged undifferentiated primary bronchial epithelial cell (PBEC) cultures (more representative of a basal-like cell type reflecting damaged epithelium) to assess the impact of CSE on autophagy and mitophagy (9, 11, 16, 24-32). Applying a more physiologically-relevant model comprised of the various epithelial cell types differentiated by culture at the air-liquid interface that allows exposure to Whole Cigarette Smoke (WCS) (including gaseous and particulate mainstream CS components) instead of an aqueous extract of CS (CSE), has the potential to provide better insight into the impact of CS on the regulation of critical mitochondrial quality control processes. Importantly, we previously reported that differentiation of PBEC at the air-liquid interface is accompanied by a marked increase in expression of genes involved in xenobiotic metabolism and increases metabolic activity (35). This is relevant for studying effects of CS exposure on PBEC cultures, because such biotransformation reactions may contribute to both detoxification of CS components as well as to formation of (more) reactive species. Therefore, comparison of such more advanced models to more simple conventional models using submerged cultures and CSE is needed to establish whether or not the use of more complex models is warranted over the use of more simple *in vitro* models.

In addition to these considerations, most available *in vitro* studies evaluated the impact of acute CS(E) exposure on mitochondrial quality control systems in airway epithelial cells. Given that COPD develops as a result of chronic exposure to CS, it is important to characterise the impact of acute *vs* chronic CS exposure on these cellular processes. Moreover, only a few *in vitro* studies investigated the long-lasting impact on parameters relevant to COPD pathophysiology after termination the CS exposure. These studies demonstrated recovery of epithelial differentiation markers (36), while inflammation (37, 38), apoptosis (39) and alterations in mitochondrial morphology and function (11) have been shown to persist upon smoking cessation *in vivo* in epithelial cells derived from former smoking COPD patients as well as in *in vitro* airway culture models. However, the impact of smoking cessation on mechanisms that underlie these (CS-induced) mitochondrial aberrations (i.e. mitochondrial biogenesis and mitophagy) are incompletely understood. In addition, if and to what extent, changes in these processes persist after smoking cessation is

unknown.

Therefore, our study investigated, for the first time, the abundance of a comprehensive panel of key regulatory molecules involved in mitochondrial metabolism in various *in vitro* models of CS exposure using human PBEC from multiple (non-COPD) donors (n=3/4 donors/model). These cells were either cultured and exposed in a submerged, undifferentiated status or were differentiated by culture in an air-liquid interface (ALI) culture system and subsequently exposed to CSE or WCS respectively. In addition to assessing the acute response of mitochondrial quality control processes to CS exposure, we also studied the impact of repeated/chronic WCS exposure during differentiation as well as recovery of mitochondria following cessation of WCS exposure in our ALI-PBEC model. This way, we obtained insight into differences and similarities between the effect of CS on the regulation of mitochondrial metabolism in 4 different epithelial culture models.

Material and Methods

PBEC isolation and expansion

PBEC of four non-COPD donors for the CSE exposure experiments of undifferentiated PBEC were provided by the Primary Lung Culture (PLUC) facility Maastricht University Medical Center+ (Maastricht, the Netherlands) and PBEC of four non-COPD donors for the WCS exposure experiments of (un-)differentiated PBEC were obtained from Leiden University Medical Center (Leiden, the Netherlands). Approval of the use of PBEC for research provided by the PLUC facility was confirmed by the scientific board of the Maastricht Pathology Tissue Collection (MPTC) under code MPTC2010-019 and the local Medical Ethic Committee code 2017-0087. PBEC were isolated, expanded and differentiated as previously described (40-43). Use of such lung tissue that became available for research within the framework of patient care at MUMC+ and LUMC was in line with the “Human Tissue and Medical Research: Code of conduct for responsible use” (2011) (www.federa.org), that describes the opt-out system for coded anonymous further use of patient data and tissue collection, storage and further use. Subject characteristics of the PBEC donors are described in Table 1.

Table 1. Characteristics of PBEC donors

Experiment	Acute WCS ALI-PBEC	Chronic WCS ALI-PBEC	Acute WCS S-PBEC	CSE-treated S-PBEC
N	4	3	3	4
Male/female	3/1	2/1	2/1	3/1
Age (years)	58.50±4.15	57.33±5.13	57.33±5.13	69.75±4.03
BMI	30.55±1.41	30.07±1.31	30.07±1.31	28±8.76
Pack years (years)	15±12.25	7.5±7.50	7.5±7.50	35±21.21**
FEV_1/FVC	70.36±5.49*	68.49±5.89*	68.49±5.89*	70.06±4.12
VC (l)	4.51±0.40	4.44±0.44	4.44±0.44	3.55±0.69

*Missing value for one donor. **Missing value for two donors. Characteristics of human PBEC donors used in the experiments: acute WCS-exposed ALI-PBEC, chronic WCS-exposed ALI-PBEC followed by smoking cessation, acute WCS-exposed S-PBEC, CSE-treated S-PBEC. Data are presented as mean±s.d. BMI, body mass index; CSE, cigarette smoke extract; FEV1, forced expiratory volume in the first second; FVC, forced vital capacity; PBEC, primary bronchial epithelial cell; VC, vital capacity; WCS, whole cigarette smoke.

In brief, PBEC were isolated from tumor-free resected bronchus rings obtained from lung cancer patients undergoing resection surgery at MUMC+ or LUMC. After isolation, PBEC were seeded and expanded in Keratinocyte-Serum Free Medium (Life-technologies Europe B.V., the Netherlands) containing 0.2 ng/ml Epidermal Growth Factor (Gibco, USA), 25 µg/ml Bovine Pituitary Extract (Gibco or Life-technologies Europe B.V.), 1 µM isoproterenol (Sigma-Aldrich, USA) and 100 µg/ml primocin (Invivogen, the Netherlands) or Mycozap (0.2%) (Lonza, USA) on 6-well plates (Corning Costar, USA) coated with 5 or 10 µg/ml human fibronectin (Promocell, Germany or Sigma-Aldrich), 30 µg/ml PureCol (Advanced BioMatrix, USA) and 10 µg/ml bovine serum albumin (BSA, Fraction V; Sigma-Aldrich or Thermo Fisher Scientific, USA) diluted in Hank's Balanced Salt Solution (HBSS; no calcium, no magnesium, no phenol red) (Gibco) or Phosphate-Buffered Saline (PBS; Fresenius Kabi, Netherlands). When cells reached confluence, cells were harvested by trypsinization and frozen in liquid nitrogen until use.

Submerged PBEC culture and CSE treatment

PBEC of four non-COPD donors ($MUMC^+$) were thawed ($5x10^5$ cells, passage 1), seeded and further expanded in supplemented Keratinocyte-Serum Free Medium medium with mycozap in pre-coated T75 flasks (Greiner Bio-One, the Netherlands) as mentioned above and previously described (42), including some minor adaptations. Subsequently, PBEC were seeded in a density of 7000 cells/cm^2 in passage 3-4 on a 12 or 24-wells plates (i.e., 1.9 or 3.8 cm^2) (Corning Costar). The next day, PBEC were washed with HBSS (no calcium, no magnesium, no phenol red) (Gibco) and cultured in Lonza Bronchial Epithelial Basal Medium supplemented with Bronchial

Epithelial Cell Growth Medium singlequots (except Gentamycin) (Lonza) and 1% Penicillin/Streptomycin (Gibco). Undifferentiated PBEC were cultured in submerged conditions (further referred as S-PBEC) for approximately three days upon 60-70% confluency. S-PBEC were starved 4 h prior treatment, by replacing the proliferation medium with starvation medium consisting of Lonza Bronchial Epithelial Basal Medium supplemented with Bronchial Epithelial Cell Growth Medium singlequots, except Gentamycin, Epidermal Growth Factor and Bovine Pituitary Extract, (Lonza) and including 1% Penicillin/Streptomycin (Gibco).

CSE was generated by using 3R4F Research Cigarettes (University of Kentucky, USA) in accordance to the protocol as previously described by Carp et al. (44). In short, after removement of the filters, a cigarette was smoked till the filter paper line by bubbling air (2 ml/sec) in HBSS (2 ml) (Gibco) using a linear pump following the regime of 5 sec smoking 10 ml, 5 sec pause. The ~4 h starved PBEC were exposed in triplicates to fresh sterile filtered CSE (1-2%) diluted in HBSS or control (HBSS; 0% CSE) in Lonza starvation medium for 4 h, 24 h or 48 h.

Submerged and ALI-PBEC culture and WCS treatment

After thawing PBEC of 4 non-COPD donors (based on pre-surgery spirometry; LUMC), cells were further expanded in supplemented Keratinocyte-Serum Free Medium medium with 1% Penicillin/Streptomycin (Gibco) replacing primocin in T75 flasks (Greiner Bio-One) as mentioned above and previously described (42). Next, 40,000 cells at passage 2 were transferred to 12-insert transwells coated with the same supplements as mentioned above. Apical and basal sides of transwells were filled with a mixture of 50% Bronchial Epithelial Cell Medium-basal (ScienCell, Sanbio) and 50% Dulbecco's modified Eagle's medium (Stemcell Technologies, Germany) (referred to as B/D medium), supplemented with 12.5 mM HEPES, bronchial epithelial cell growth supplement, 100 U/ml penicillin, 100 ug/ml streptomycin (all from ScienCell), 2 mM glutaMAX (Thermo Fisher Scientific). During submerged PBEC culture, the medium was supplemented with 1 nM of the synthetic retinoid EC23 (Tocris, Abingdon, UK). Undifferentiated PBEC were cultured in submerged conditions (further referred as S-PBEC) for about six days to reach confluence before WCS or air exposure, or cultured at the ALI to induce mucociliary differentiation (referred to as ALI-PBEC) as previously described (45). After confluence was reached, the apical medium was removed and cells were cultured at the ALI in B/D medium as described above with 50 nM EC23 for 2 weeks; three times a week the basal medium was refreshed and the apical side was washed with PBS to remove excess mucus.

For WCS exposure, S-PBEC or ALI-PBEC cultures cultured on transwells were exposed to either fresh air (control) or WCS from one research cigarette 3R4F (University of Kentucky) using an exposure chamber specifically designed for cell

culture experiments as previously described (46). In S-PBEC, apical medium was removed shortly before WCS exposure. Fresh air or WCS derived from one cigarette in the holder was pumped into the exposure chamber until one cigarette burned out. After that, fresh air was used to remove residual WCS from the chamber for 10 min. The weight difference of a filter placed between the pump and exposure chamber before and after exposure was recorded to measure the amount of smoke infused inside the exposure chamber. Approximately 2 mg cigarette smoke–derived particles were deposited on the filter as determined by measuring the filter of different exposures. After WCS or air exposure, apical medium was added to undifferentiated cultures. Cultures were harvested at 6 h and 24 h after exposure according to experimental requirements.

For chronic WCS exposure and cessation, after reaching confluence on the inserts, ALI-PBEC were apically washed every day to remove mucus at 4 h prior to daily WCS exposure and exposed to either fresh air or WCS during differentiation at the ALI for a total of 14 days (chronic exposure model), followed up by a cessation period of 10 days. Cells and basal medium were harvested on ALI-Day 14, 16, 19 and 23 to isolate proteins and mRNA as well as measure the levels of L-lactate.

Separation of luminal and basal cell-enriched fractions

ALI-PBEC were separated into luminal and basal cell fractions at 6 h after WCS or air exposure as described previously, using calcium depletion followed by trypsinization (46). Successful separation was identified by measuring gene expression of a basal cells marker (TP63) and an early progenitor cell marker (cytokeratin-8, KRT8).

RNA isolation, cDNA synthesis and real time quantitative PCR analysis

CSE-treated undifferentiated PBEC were lysed after 4 h, 24 h or 48 h in 200-400 µL RLT lysis buffer including 1% 2-Mercaptoethanol (Sigma-Aldrich) and processed according to the RNeasy® Mini Kit manufacturer's protocol (Catalog number 74104 and 74106, Qiagen, USA). WCS-exposed S-PBEC or ALI-PBEC were lysed using RNA lysis buffer and total RNA was robotically isolated using Maxwell® 16 simply RNA tissue kit (Promega, the Netherlands). The NanoDrop ND 1000 UV-visible spectrophotometer (Isogen Life Sciences, the Netherlands or Nanodrop Technologies, USA) was used to analyze the quantity and purity of the RNA samples. Total RNA (CSE experiments: 25-140 ng; WCS experiments: 500 ng) was reverse transcribed using iScript™ cDNA synthesis method (Bio-Rad, the Netherlands). The cDNA was diluted in milliQ (CSE:1:17.86-1:100; WCS:1:50) in order to have an equal original input of 25 or 10 ng RNA per experiment and stored at -20°C until further analysis.
Expression of genes of interest was analyzed in all samples by real time quantitative PCR (qPCR) by mixing diluted cDNA, target- and human-specific primers (Eurofins, the

Netherlands or Invitrogen, USA) and 2xSensiMix™ SYBR® & Fluorescein Kit (Bioline, the Netherlands) or IQ SYBR green Supermix (Bio-Rad) in white 384 multiwell plates (Roche, Switzerland or BIOplastics BV, the Netherlands). Subsequently, the thermal cycling protocol (10 min at 95°C, 55 cycles of 10 seconds at 95°C, 20 seconds at 60°C) was run on a Roche LightCycler 480 machine (Roche). The following software programs were used to perform melt curves and gene expression analysis: LightCycler480 software (Roche) and LinRegPCR software 2014.x (the Netherlands), respectively. Moreover normalization of the expression of mRNA transcripts of interest was conducted by using GeNorm software 3.4 (Primerdesign, USA) which calculated a correction factor based on the expression of a combination of reference genes (*ACTB, B2M, PPIA, RPL13A, ATP5B*). A list of used target and human specific primer sequences is shown in Table S1.

DNA isolation and mitochondrial DNA copy number analysis

Following exposures, CSE was kept with the cells for 24 or 48 h, or cells were cultured for 6 h or 24 h after short WCS treatment. Next, PBEC were lysed in 250-400 µl lysis buffer (0.1 M Tris/HCl pH 8.5, 0.005 M EDTA pH 8.0, 0.2% (w/v) sodium dodecyl sulphate, 0.2 M NaCl) at room temperature. To isolate DNA, addition of Proteinase K (10 mg/ml) (Qiagen) to the lysates (1:50) was required, followed by overnight incubation at 55°C. The next day, lysates were centrifuged at 20,000 x g for 15 min. Thereafter, 500 µl isopropanol was added to the supernatant facilitating DNA precipitation by vigorously shaking. Following two washes of the DNA pellets with 70% ethanol, dry DNA pellets were dissolved in 125 µl TE-Buffer (10 mM Tris/HCl pH 8.0, 1 mM EDTA). The DNA samples were subsequently incubated at 55°C for 2 h, overnight at 4°C and finally stored at -20 °C until use. DNA quantity and purity was determined by using the NanoDrop ND 1000 UV-vis spectrophotometer (Isogen Life Sciences). DNA samples were diluted in TE-buffer (1:50) followed by qPCR analysis (see paragraph 2.3). Mitochondrial DNA (mtDNA) copy numbers were assessed by investigation the ratio of the expression of mtDNA, Mitochondrially-Encoded Cytochrome C Oxidase II (*MT-CO2*), and genomic DNA, *ACTB* (Table S1).

Western Blotting

Whole cell lysates for western blotting were generated by lysis of treated PBEC in 200 µL Whole Cell Lysis buffer (20 mM Tris pH 7.4, 150 mM NaCl, 1% Nonidet P40 in MilliQ) or Pierce RIPA buffer (Thermo Fisher Scientific,) including fresh PhosSTOP Phosphatase and cOmplete, Mini, EDTA-free protease inhibitor cocktail tablets (both Roche). The whole cell lysates were rotated and subsequently centrifuged at 20,000 x g both for 30 min at 4°C. Assessment of the total protein content in the whole cell lysate fraction was conducted according to the manufacturer's protocol of the Pierce™ BCA Protein Assay Kit range 20-2000 µg/mL (Thermo Fisher Scientific). The

whole cell lysate supernatant was consecutively diluted to similar concentration within experiments (range 0.0667-1 µg/µl) in a final concentration of 1x Laemmli buffer (0.25 M Tris pH 6.8, 8% (w/v) sodium dodecyl sulphate, 40% (v/v) glycerol, 0.4 M Dithiothreitol, 0.02% (w/v) Bromophenol Blue), boiled at 100°C for 5 min and stored at -80°C pending analysis.

Samples (1-10 µg of protein per lane) and at least two protein ladders (Precision Plus Protein™ All Blue Standards #161-0373, Bio-Rad) were run on each gel in 1x MES running buffer (Bio-Rad) on a Criterion XT Precast 4-12 or 12% Bis-Tris gel (Bio-Rad). Separation of the proteins was achieved by electrophoresis (100-130 V for 1 h), followed by electroblotting (Bio-Rad Criterion Blotter) (100 V for 1 h) to transfer the proteins from the gel to a 0.45 µM Nitrocellulose Transfer membrane (Bio-Rad). To quantify total protein content, the nitrocellulose membranes were stained using 0.2% (w/v) Ponceau S in 1% (v/v) acetic acid (Sigma-Aldrich) for 5 min, followed by a milliQ wash and imaging using the Amersham™ Imager 600 (GE Healthcare, the Netherlands). After removal of the Ponceau S staining, non-specific binding sites on the membranes were blocked for 1 h in 3% (w/v) non-fat dry milk (Campina, the Netherlands) in Tween20 Tris-buffered saline (TBST; 20 mM Tris, 137 mM NaCl, 0.1% (v/v) Tween20, pH 7.6). Subsequently, a TBST wash was followed by overnight incubation of the membranes at 4°C with a target-specific primary antibody (Table S2) diluted 1:500-1:1000 in TBST with 3% (w/v) BSA or non-fat dry milk. The next day, membranes were washed and incubated with a horseradish peroxidase-conjugated secondary antibody (Table S2) diluted 1:10,000 in 3% (w/v) non-fat dry milk in TBST for 1 h at room temperature. Thereafter, membranes were washed again and incubated for 3 min with either 0.25 x Supersignal West FEMTO or 0.5 x Supersignal West PICO Chemiluminescent Substrate (Thermo Fisher Scientific) to visualize the target proteins using the Amersham™ Imager 600 (GE Healthcare). Quantification of images was performed using Image Quant software (GE Healthcare). Absolute protein quantification was calculated by correcting for total protein loading content assessed by Ponceau S Staining over the entire size range of proteins (250 kDa - 10 kDa). The western blot images presented in the figures of this manuscript have been equally adjusted for brightness and contrast throughout the picture. Selected images reflecting changes in one PBEC donor are representative for the group of donors/experiment (n=3/4 donors/experiment).

Metabolic enzyme activity assays

Metabolic enzyme activity lysates were generated by lysis of treated PBEC in 100 µl 0.5% Triton X-100 (Sigma-Aldrich) for 15 min on ice, followed by scraping (on ice). Subsequently, the lysates were centrifuged at 20,000 x g for 2 min at 4°C. Supernatants were aliquoted for protein analysis or diluted in 5% BSA in milliQ (1:4) for metabolic enzyme activity analysis, both stored at -80°C. Total protein content

in the supernatant fraction was evaluated following the manufacturer's protocol of the Pierce™ BCA Protein Assay Kit range 20-2000 µg/mL (Thermo Fisher Scientific).

After running the three assays (Citrate synthase, Hydroxyacyl-Coenzyme A Dehydrogenase (HADH) and Phosphofructokinase 1 (PFK 1), analysis of the samples was spectrophotometrically conducted at 340 nM (HADH/PFK 1) or 412 nM (Citrate synthase) at 37°C using the Multiskan Spectrum plate reader (Thermo Labsystems, the Netherlands). Enzyme activity was calculated by slope determination and correction for total protein content of the samples. Details of the analyses were as follows:

Citrate synthase. Citrate synthase activity was assessed as previously described (EC 2.3.3.1) (47) by mixing undiluted samples with reagent (100 mM Tris, 0.1 mM DNTB, 40 µM acetyl coenzyme A), followed by initiation of the reaction by addition of oxaloacetic acid (25 mM).

HADH. HADH enzyme activity was assessed as previously described (EC 1.1.1.35) (48). After mixing the undiluted samples with reagent (0.22 mM NADH, 100 mM tetrapotassium pyrophosphate pH 7.3), the reaction was initiated by addition of 2.3 mM acetoacetyl-CoA.

PFK 1. As previously described (EC 2.7.1.11) (49), PFK 1 enzyme activity was evaluated by mixing undiluted samples with reagent (48.8 mM Tris, 7.4 mM $MgCl_2.6H_2O$, 74 mM KCl, 384 µM KCN, 2.8 mM ATP, 1.5 mM DTT, 0.3 mM NADH, 0.375 U/mL aldolase, 0.5625 U/mL glycerol-3-phosphate dehydrogenase and 7.425 U/mL triose phosphate isomerase, pH 8.0). To initiate the reaction, fructose-6-phosphate (30.6 mM) in Tris buffer (49.5 mM, pH 8.0) was added to the mix of undiluted sample and reagent.

Lactate assay

Levels of L-lactate in apical and basal medium collected from S-PBEC and the basal medium of ALI-PBEC at 24 h after acute/chronic WCS exposure were measured using the Lactate Colorimetric/Fluorometric Assay Kit (K607-100, BioVision, USA). In brief, 50 µl diluted samples in Lactate Assay Buffer were mixed with 50 µl Reaction Mix (Lactate Enzyme Mix, Probe and Lactate Assay Buffer) and incubated for 30 min. The absorbance at OD 570 nm was measured in a microplate reader (Bio-Rad).

Immunofluorescence staining and confocal microscopy

Immunofluorescence staining of ALI-PBEC cultures on inserts was performed as mentioned before (45). At indicated time points after acute WCS exposure, membranes with attached ALI-PBEC were washed and PBEC fixed in 4% (w/v)

paraformaldehyde in PBS for 30 min at room temperature. Membranes were washed once and stored in PBS at 4°C until use. Before staining for intracellular antigens, ice cold methanol was added for 10 min at 4°C. Blocking and permeabilization buffer for non-specific binding sites was PBS/1% (w/v) BSA/0.3% (w/v) Triton-X-100 (PBT) buffer. After incubation for 30 min at 4°C, specific binding sites were stained with rabbit anti-LC3B antibody (1:100; Cell Signaling Technology, USA) together with mouse anti-MUC5AC antibody (1:200; Thermo Fisher Scientific), anti-acetylated α-tubulin antibody (1:500; Sigma-Aldrich), anti-CC-10 antibody (1:50; Hycult Biotech, the Netherlands) or anti-NGFR antibody (1:100; Abcam, UK) for 1 h at room temperature. After washing, secondary antibodies (donkey anti-rabbit and donkey anti-mouse Alexa-flour antibodies; all diluted 1:200, Thermo Fisher Scientific) and 4',6-diamidino-2-phenylindole (DAPI, 1:50, Sigma-Aldrich) were added to the cells in the dark for 30 min at room temperature. Next, membranes with ProLong™ Gold Antifade Mountant (Thermo Fisher Scientific) were placed on glass slides and covered with a coverslip. Slides were viewed using a Leica TCS SP8 confocal microscope (Leica Microsystems, Germany) at 630 x original magnification.

Statistical analysis

GraphPad Prism 8.0.1 software (La Jolla, USA) was used to perform statistical analyses and graph the data. Data are presented as mean fold change compared to control (air, 0% CSE or Day 14) ± standard error of the mean (SEM). Statistical testing of differences between acute WCS *versus* air exposures in S-PBEC or ALI-PBEC was performed by using a two-tailed paired parametric t-test. Moreover, a two-tailed paired parametric t-test was conducted to test differences in WCS *versus* air exposures after smoking cessation in ALI-PBEC on each day (e.g., WCS Day 14 versus air control). If comparison of various groups was required in case of the CSE exposure (CSE 1% or 2% *versus* 0% CSE) or in WCS chronic smoking cessation experiments (WCS Day 16, 19, 23 *versus* WCS Day 14), assuming a Gaussian distribution and using Geisser-Greenhouse correction, an one-way ANOVA (matched/repeated measures) followed by Sidak's post-hoc test for multiple comparisons was conducted, and in case of missing values the mixed-effects models was performed. Statistical significance was considered if p-values were below 0.05 ($^{*}p<0.05$) or 0.01 ($^{**}p<0.01$) and a trend was indicated if $^{\#}p<0.1$.

Results

We deployed four models of exposure of PBEC to WCS or CSE. These included respectively A) differentiated ALI-PBEC acutely-exposed to WCS, B) ALI-PBEC chronically-exposed (during differentiation) to WCS followed by smoking cessation, C) undifferentiated S-PBEC acutely-exposed to WCS and D) undifferentiated S-PBEC treated with CSE (Fig. 1). ALI-PBEC cultures were differentiated and included

several distinct cell types present in the pseudostratified epithelium mimicking the 'healthy' normal airway epithelium (36). Undifferentiated S-PBEC on the other hand consisted of basal cells, reflecting injured/damaged airway epithelium. Collectively, these models allowed us not only to test our hypothesis that WCS exposure has a differential impact on mitochondrial quality control systems in undifferentiated (predominantly basal-like cell type) *versus* differentiated (including ciliated, club and goblet cells) human PBEC cultures, but also allowed us to compare the effect of an aqueous extract of CS (CSE) to that of WCS (particles and gaseous components) and assess the potential influence of smoking cessation.

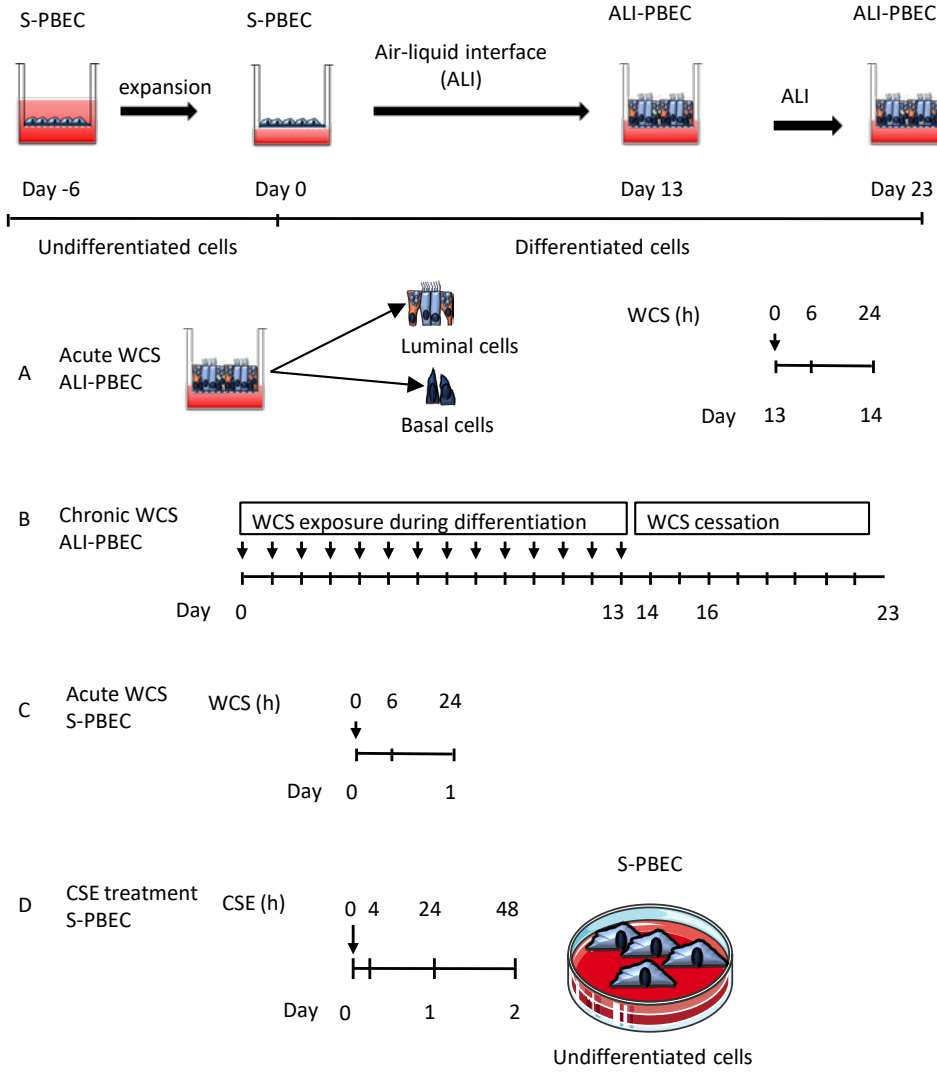

Figure 1. Experimental cigarette smoke-exposed cell models. Models A, B and C were cultured on transwells to allow apical exposure to fresh air or WCS, whereas the model shown in D was cultured on tissue culture plastic requiring submerged exposure to CSE. **(A)** Acute WCS-exposed ALI-PBEC: after 2-weeks of differentiation, ALI-PBEC were exposed to fresh air or WCS from one 3R4F cigarette (University of Kentucky, 2 mg). Subsequently, whole cell lysates or basal and luminal cell fractions were harvested after 6 h and 24 h, or only at 6 h post-exposure, respectively (n=3 donors/group). **(B)** Chronic WCS-exposed (during differentiation) ALI-PBEC followed by smoking cessation: ALI-PBEC were 1x daily exposed to fresh air or WCS from one 3R4F cigarette (University of Kentucky, 2 mg) during differentiation for 14 days followed by a cessation period up to 10 days. Cells were harvested on Day 14 (24 h after the last WCS exposure), 16, 19 and 23 (n=3 donors/group). **(C)** Acute WCS-exposed S-PBEC: Undifferentiated S-PBEC were exposed, after removal of apical medium, to fresh air or WCS from one 3R4F cigarette (University of Kentucky, 2 mg) followed by harvesting of whole cell lysates after 6 h and 24 h recovery (n=3 donors/group). **(D)** CSE-treated S-PBEC: Undifferentiated S-PBEC were submerged treated with CSE from one 3R4F cigarette (University of Kentucky) diluted in HBSS (0-1-2%) in Lonza starvation medium for 4 h, 24 h or 48 h (n=4 donors/group)**.**

Increase in autophagy markers in response to CS exposure

As autophagy proteins play a key role in facilitating mitochondrial quality control (i.e. breakdown) by the autophagosomal pathways, we studied the effect of WCS exposure in ALI-PBEC on the abundance of several autophagy-related proteins. Firstly, as it has been reported that activation of autophagy, as a cytoprotective mechanism, is related to oxidative stress (50), and to verify that our CS exposures were able to elicit a cellular response indicative of successful exposure in the different models, we investigated the oxidative stress response to WCS or CSE by measuring anti-oxidant gene expression in our four models. Elevated mRNA levels of superoxide dismutase 1 (*SOD1*) were observed in ALI-PBEC following acute WCS exposure and 24 h after chronic WCS exposure during differentiation (Figs S1A, C). Separation of cellular fractions revealed that the acute WCS-induced upregulation of *SOD2* expression originated from both the luminal and basal cell fraction (Fig. S1B). The separation of basal and luminal cell fractions was validated by measuring gene expression of basal cell marker *TP63* and early progenitor cell marker *KRT8* (Fig. S2) respectively. In contrast to changes observed in ALI-PBEC exposed to WCS, in S-PBEC exposed to CSE only *SOD1* transcript levels were induced (in a dose-dependent manner) while *SOD2* transcript abundance was decreased, which was not observed in S-PBEC exposed to WCS (Fig. S1D).

Our previous results also showed that acute WCS exposure resulted in increased expression of genes involved in the antioxidant defense, including heme oxygenase 1 and NAD(P)H quinone oxidoreductase 1 in ALI-PBEC (51). In accordance with these previous data, our results collectively point to a cellular response to oxidative stress indicative of successful exposure to CS(E) in the different models.

Next, we assessed the impact of exposure of the cells to CS constituents on the

abundance of autophagy-related proteins. As shown in Figs 2A, B, C, both protein and transcript levels of the adaptor proteins SQSTM1 and GABARAPL1, as well as the marker of the accumulation of autophagosomes (LC3BII), were increased after WCS exposure in ALI-PBEC. These increases were most pronounced at 6 h post-WCS exposure and were largely dissipated after 24 h. Similar results were obtained in S-PBEC exposed to WCS or CSE (Fig. S3), although it appeared that induction in transcript abundance of autophagy markers in response to CSE was delayed and more pronounced compared to these changes in ALI-PBEC cultures stimulated with WCS (Fig. S3C). Importantly, to further determine the cellular location of the increased expression of these autophagy markers in response to WCS, we isolated basal and luminal cells from WCS-exposed ALI-PBEC cultures. By comparison, both basal and luminal cell fractions of ALI-PBEC expressed higher mRNA levels of autophagy markers after WCS exposure indicating that both fractions were similarly affected by WCS exposure (although responses appeared to be slightly more pronounced in the basal fraction) (Fig. 2D). To further investigate and validate these findings, an immunofluorescence assay was conducted, using staining with the anti-LC3B antibody as autophagy indicator; co-staining with anti-MUC5AC, anti-acetylated α-tubulin, anti-CC-10 and anti-NGFR was used to detect goblet cells, ciliated cells, club cells and basal cells, respectively. As depicted in Fig. 2E, presence of cell differentiation markers demonstrates differentiation of air and WCS exposed PBEC in our model. WCS exposure enhanced the number of $LC3B^{+}$ puncta in ALI-PBEC (Fig. 2E), which was most pronounced in basal cells and goblet cells. Furthermore, the pronounced induction in abundance of autophagy markers in acute WCS models was largely absent in the chronic WCS-exposed ALI-PBEC cultures. Moreover, even a decreased ratio of LC3BII/I was observed 24 h after the last exposure which was recovered after WCS cessation (Figs 2F, G, H).

Taken together, acute WCS exposure of well differentiated ALI-PBEC (representing an intact epithelial layer) resulted in an elevated abundance of autophagy markers associated with accumulation of autophagosomes and expression of ubiquitin-binding autophagic adaptors localized in both basal and luminal cells. Similar findings were made in undifferentiated S-PBEC exposed to CSE or WCS (representing damaged epithelium). Importantly, these changes were reversible as they were no longer observed after cessation in our chronic ALI-PBEC WCS exposure model.

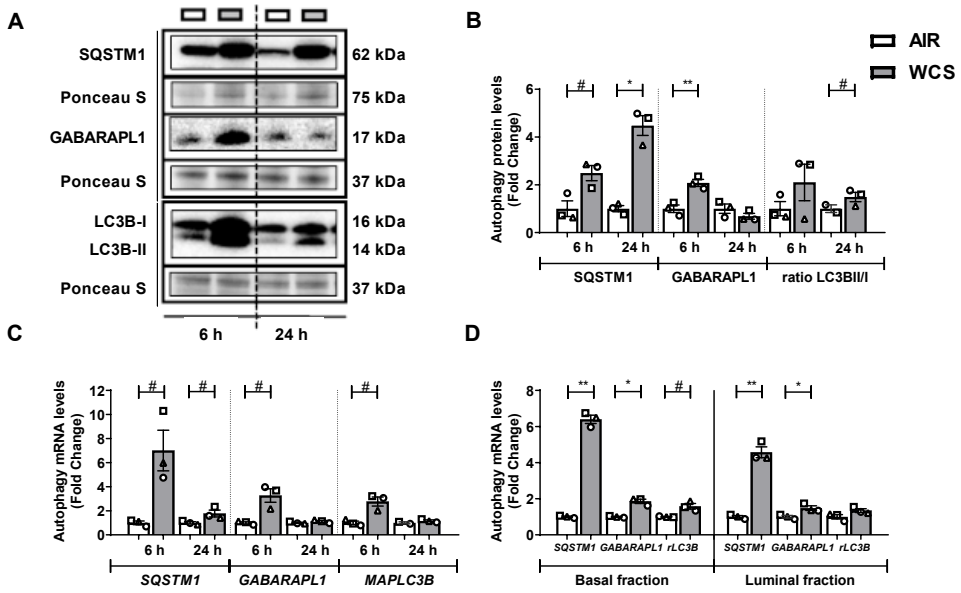
A
SQSTM1
Ponceau S
GABARAPL1
Ponceau S
LC3B-I
LC3B-II
Ponceau S
62 kDa
75 kDa
17 kDa
37 kDa
16 kDa
14 kDa
37 kDa
6 h
24 h
B
AIR
WCS
Autophagy protein levels (Fold Change)
SQSTM1
GABARAPL1
ratio LC3BII/I
C
Autophagy mRNA levels (Fold Change)
SQSTM1
GABARAPL1
MAPLC3B
D
Autophagy mRNA levels (Fold Change)
SQSTM1
GABARAPL1
rLC3B
Basal fraction
Luminal fraction

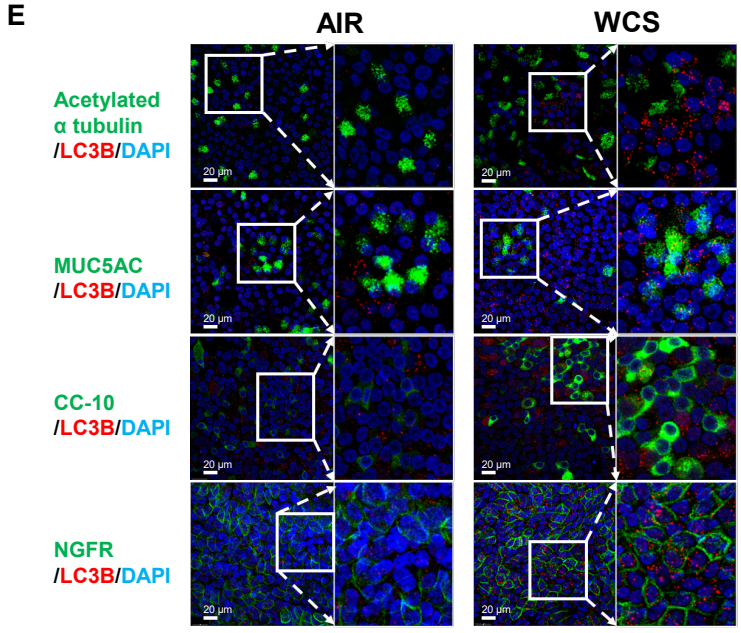
E
AIR
WCS
Acetylated α tubulin /LC3B/DAPI
MUC5AC /LC3B/DAPI
CC-10 /LC3B/DAPI
NGFR /LC3B/DAPI
20 µm

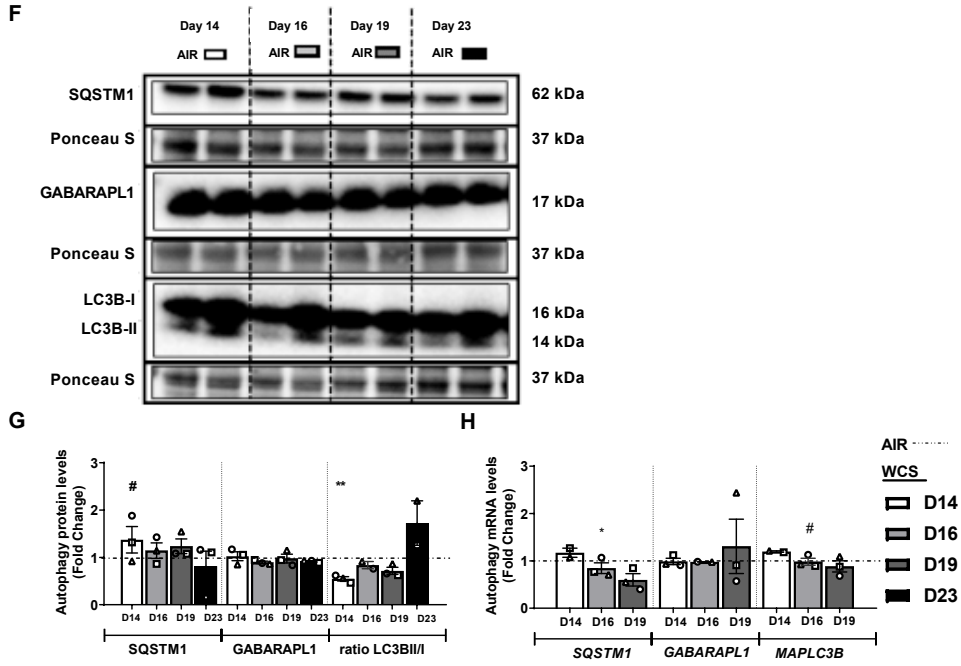

Figure 2. Increase in abundance of autophagy markers in WCS-exposed ALI-PBEC. After 2-weeks of differentiation, ALI-PBEC were exposed to fresh air or WCS from one 3R4F cigarette (University of Kentucky, 2 mg) and whole cell lysates or basal and luminal cell fractions were harvested after 6 h and 24 h or only 6 h post-exposure, respectively (n=3 donors/group). Protein abundance (A, B) as well as transcript abundance (C, D) of autophagy regulators SQSTM1, GABARAPL1 and ratio LC3BII/I or MAP1LC3B in whole cell lysates or in basal/luminal cell fractions post exposure are presented. Immunofluorescence staining and confocal microscopy was conducted post WCS exposure in differentiated ALI-PBEC using antibodies for anti-LC3B (red) together with anti-MUC5AC (green), anti-acetylated α-tubulin (green), anti-CC-10 (green) and anti-NGFR (green) in combination with 4',6-diamidino-2-phenylindole (DAPI) (blue) for nuclear staining. Immunofluorescence images shown are representative for 3 donors with 630 x original magnification (E). ALI-PBEC were 1x daily exposed to fresh air or WCS from one 3R4F cigarette (University of Kentucky, 2 mg) during differentiation for 14 days followed by a cessation period up to 10 days. Cells were harvested on Day 14 (24 h after the last exposure), 16, 19 and 23 (n=3 donors/group). Protein (F, G) and mRNA levels (H) of autophagy regulators SQSTM1, GABARAPL1 and ratio LC3BII/I or MAP1LC3B were analyzed in whole cell lysates. Representative western blots are shown. Data are presented as mean fold change compared to control (air or WCS Day 14) ± SEM. Statistical significance is indicated as $^{\#}p<0.1$, $^{*}p<0.05$ and $^{**}p<0.01$ compared to control (air or WCS Day 14).

Modulation of mitophagy-specific markers in response to CS exposure

Since we observed a potent increase in the abundance of general autophagy markers in response to WCS exposure and because these proteins are also essential for

mitochondrial-specific autophagy (mitophagy), we next investigated if the specific receptor- and ubiquitin-mediated mitophagy pathways involved in the removal of damaged or dysfunctional mitochondria, were also affected by WCS exposure.

As illustrated in Fig. 3, protein levels of BNIP3 and mRNA levels of *BNIP3L* and *FUNDC1* were significantly increased 24 h after acute WCS exposure in differentiated ALI-PBEC (Figs 3A, B, C). In contrast, we observed a transient decrease in mRNA levels of *FUNDC1* at 6 h post-WCS exposure in these cultures (Fig. 3C). To study the impact of acute WCS exposure on regulators of mitophagy in specific epithelial cell types, we also investigated transcript levels of those regulators in the basal and luminal fractions of these differentiated ALI-PBEC cultures at 6 h post WCS exposure. In line with the whole cell lysate data, increased *BNIP3*(*L*) and decreased *FUNDC1* mRNA expression were observed in both fractions (Fig. 3D). The chronic WCS exposure model revealed that increases in BNIP3 protein levels in response to WCS were persistent 24 h after chronic WCS exposure whereas changes in the transcript abundance of other regulators of mitophagy were more transient in nature (Figs 3E, F, G). Although CSE exposure of undifferentiated S-PBEC yielded similar results as in ALI-PBEC cultures (i.e. increased BNIP3 protein), WCS exposure of these cells revealed only significantly decreased BNIP3 mRNA levels (Fig. S4).

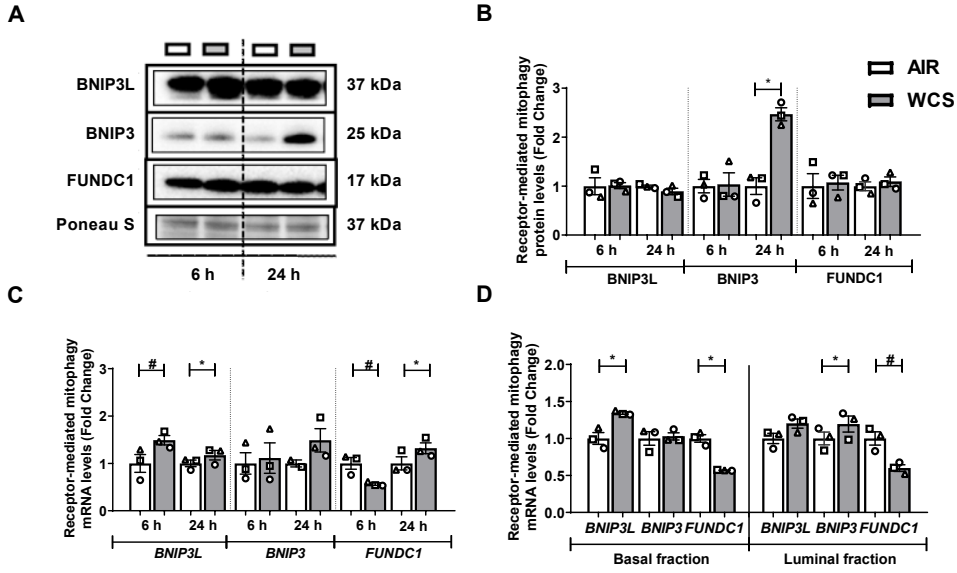

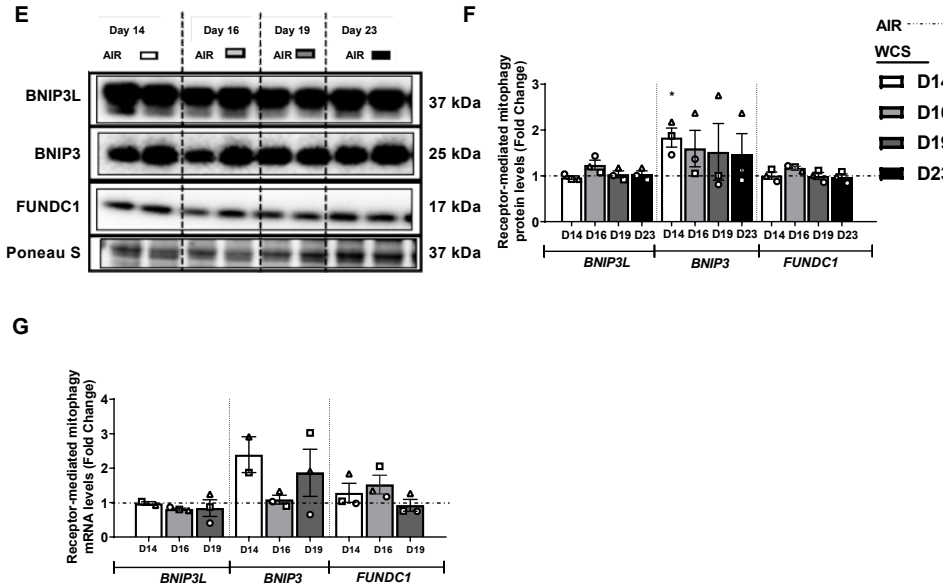

Figure 3. WCS-induced changes in protein and mRNA levels of constituents involved in the receptor-mediated mitophagy machinery in ALI-PBEC. After 2-weeks of differentiation, ALI-PBEC were exposed to fresh air or WCS from one 3R4F cigarette (University of Kentucky, 2 mg) and whole cell lysates or basal and luminal cell fractions were harvested after 6 h and 24 h or only 6 h post-exposure, respectively (n=3 donors/group). Protein **(A, B)** as well as mRNA levels **(C, D)** of constituents involved in receptor-mediated mitophagy BNIP3L, BNIP3, FUNDC1 were analyzed in whole cell lysates or basal/luminal cell fractions post exposure. ALI-PBEC were 1x daily exposed to fresh air or WCS from one 3R4F cigarette (University of Kentucky, 2 mg) during differentiation for 14 days followed by a cessation period up to 10 days. Cells were harvested on Day 14 (24 h after the last exposure), 16, 19 and 23 (n=3 donors/group). Protein **(E, F)** and mRNA levels **(G)** of receptor-mediated mitophagy regulators BNIP3L, BNIP3, and FUNDC1 were analyzed in whole cell lysates. Representative western blots are shown. Data are presented as mean fold change compared to control (air or WCS Day 14) ± SEM. Statistical significance is indicated as $^{\#}p<0.1$, $^{*}p<0.05$ and $^{**}p<0.01$ compared to control (air or WCS Day 14) .

Since the abundance of the ubiquitin-binding autophagic adaptor SQSTM1 was increased in response to acute WCS exposure (Fig. 2), we further investigated the expression levels of ubiquitin-dependent mitophagy regulators PINK1 and PRKN. In general, PRKN abundance was significantly decreased in response to acute WCS exposure in ALI-PBEC and upon CSE treatment in S-PBEC, whereas PINK1 protein and transcript levels showed a trend to increase in acute WCS-exposed ALI-PBEC as well as upon smoking cessation (Figs 4 and S5).

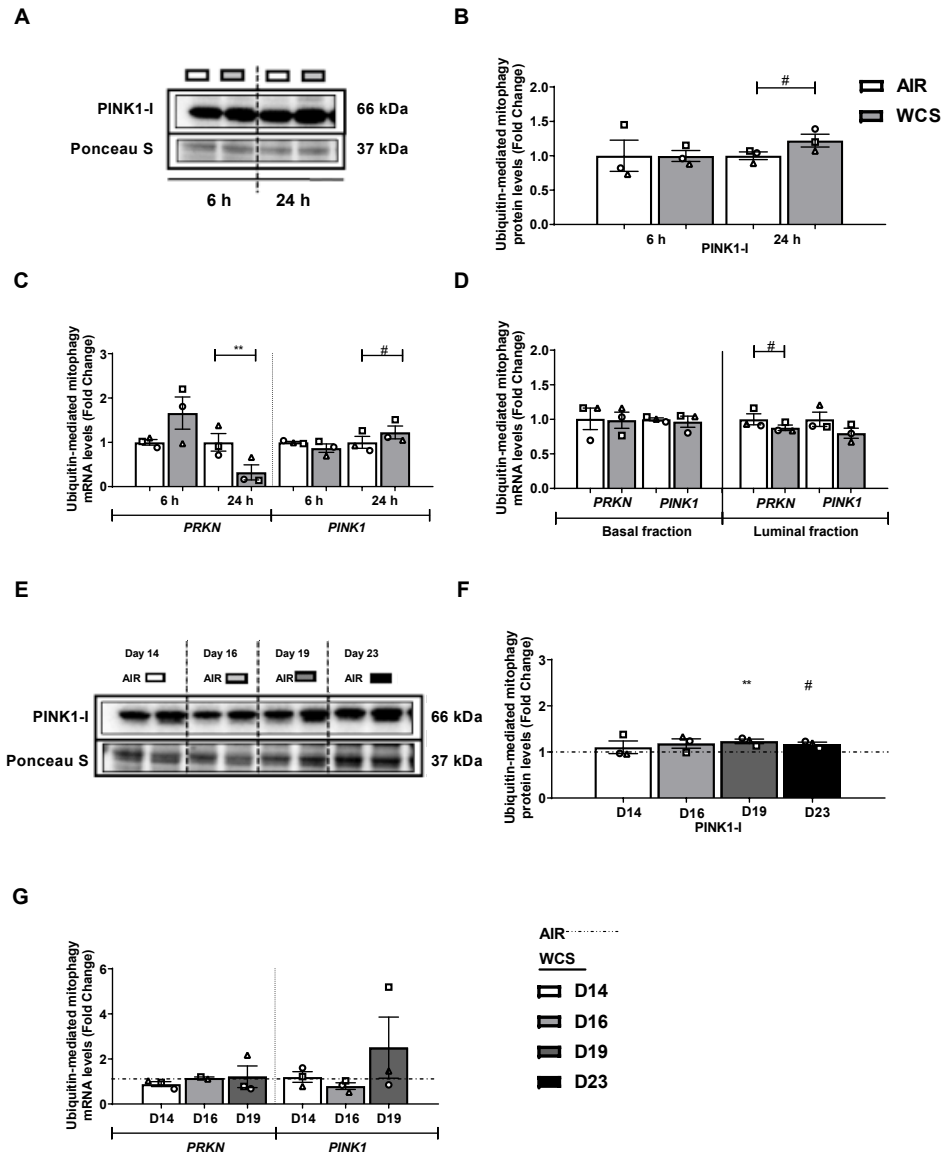

Figure 4. Alterations in the abundance of constituents associated with ubiquitin-mediated mitophagy in ALI-PBEC. After 2-weeks of differentiation, ALI-PBEC were exposed to fresh air or WCS from one 3R4F cigarette (University of Kentucky, 2 mg) and whole cell lysates or basal and luminal cell fractions were harvested after 6 h and 24 h or only 6 h post-exposure, respectively (n=3 donors/group). Protein **(A, B)** as well as mRNA levels **(C, D)** of constituents involved in ubiquitin-mediated mitophagy PRKN and PINK1 were analyzed in whole cell lysates or basal/luminal cell fractions post exposure. ALI-PBEC were 1x daily exposed to fresh air or WCS from one 3R4F cigarette (University of Kentucky, 2 mg) during differentiation for 14 days followed by a cessation period up to 10 days. Cells were harvested on Day 14 (24 h after the last exposure), 16, 19 and 23 (n=3 donors/group). Protein **(E, F)** and mRNA levels

(G) of mitophagy regulators PRKN and PINK1 were analyzed in whole cell lysates. Western blot analysis revealed two distinct bands corresponding with expected molecular weights for PINK protein, entitled PINK1-I (66 kDa) and PINK1-II (55 kDa). Representative western blots are shown. Data are presented as mean fold change compared to control (air or WCS Day 14) ± SEM. Statistical significance is indicated as $^{\#}p<0.1$, $*p<0.05$ and $**p<0.01$ compared to control (air or WCS Day 14).

In conclusion, these results indicate that WCS as well as CSE stimulation specifically affects the regulation of receptor-mediated mitophagy which was consistently observed in all models and, at least to some degree persists upon chronic WCS exposure and smoking cessation.

WCS-induced alterations in the molecular machinery controlling mitochondrial biogenesis

As both mitophagy and mitochondrial biogenesis play an essential role in maintaining mitochondrial homeostasis, we next investigated the impact of CS on the abundance of constituents involved in the genesis of mitochondria.

Firstly, in ALI-PBEC, we evaluated whether acute WCS exposure affected the abundance of transcriptional co-activators of the PPARGC1 network, a critical signaling cascade involved in the regulation of mitochondrial biogenesis and mitochondrial energy metabolism (20). No significant changes were observed in protein and transcript levels of most investigated transcriptional co-activators of the PPARGC1 network (i.e. PPARGC1A and PPARGGC1B) in whole cell lysates in all models (Figs 5 and S6). However, elevated Peroxisome Proliferator-Activated Receptor Gamma Coactivator-Related Protein 1 (*PPRC1*) mRNA levels were observed in response to acute WCS exposure in both basal and luminal fractions of WCS-exposed ALI-PBEC (Fig. 5D). A similar response, although not all statistically-significant, likely due to interdonor variation, was observed in whole cell lysates after WCS-exposure of both differentiated ALI-PBEC and undifferentiated S-PBEC (Figs 5C and S6C). Remarkably, abundance of *PPARGC1B* mRNA levels showed a transient response to acute WCS exposure while we observed a decline in response to CSE in S-PBEC (Figs. 5C, D and S6C). In contrast to acute WCS exposure, PPARGC1A mRNA levels were significantly decreased upon chronic WCS exposure (Fig. 5G).

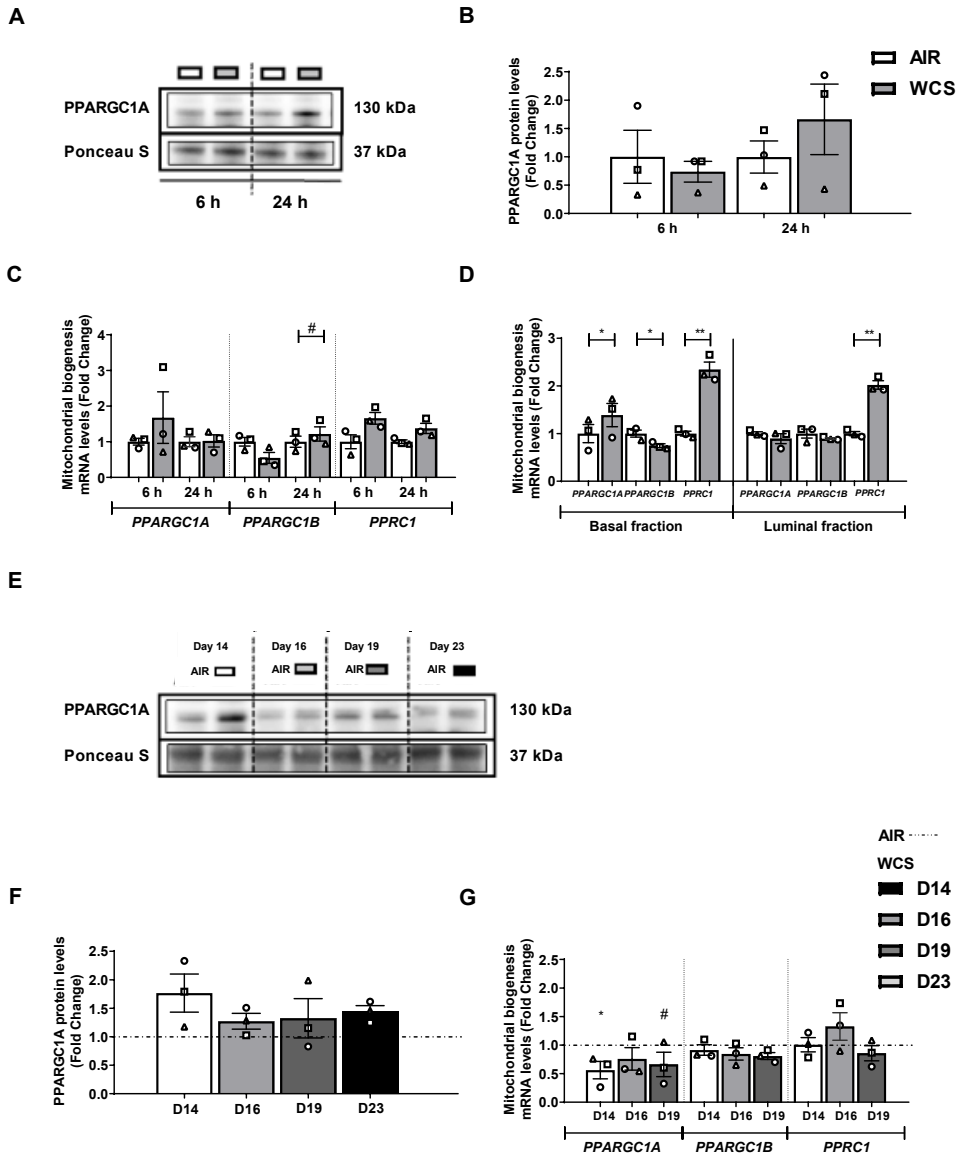

Figure 5. Changes in transcription factors associated with mitochondrial biogenesis in response to WCS exposure in ALI-PBEC. After 2-weeks of differentiation, ALI-PBEC were exposed to fresh air or WCS from one 3R4F cigarette (University of Kentucky, 2 mg) and whole cell lysates or basal and luminal cell fractions were harvested after respectively 6 h and 24 h or only 6 h post-exposure, respectively (n=3 donors/group). Protein **(A, B)** as well as mRNA abundance **(C, D)** of transcriptional co-activators of the PPARGC1 network, i.e. PPARGC1A, PPARGC1B and PPRC1, were analyzed in whole cell lysates or basal/luminal cell fractions post exposure. ALI-PBEC were 1x daily exposed to fresh air or WCS from one 3R4F cigarette (University of Kentucky, 2 mg) during differentiation for 14 days followed by a

cessation period up to 10 days. Cells were harvested on Day 14 (24 h after the last exposure), 16, 19 and 23 (n=3 donors/group). Protein **(E, F)** and mRNA levels **(G)** of indices involved in the PPARGC1 network are depicted. Representative western blots are shown. Data are presented as mean fold change compared to control (air or WCS Day 14) ± SEM. Statistical significance is indicated as $^{\#}p<0.1$, $^{*}p<0.05$ and $^{**}p<0.01$ compared to control (air or WCS Day 14).

Thereafter, we examined the impact of WCS exposure on abundance of transcription factors associated with the PPARGC1 network. Protein and transcript levels of PPARGC1-coactivated transcription factors, either Transcription Factor A, Mitochondrial (TFAM), Nuclear Respiratory Factor 1 (NRF1) or Estrogen Related Receptor Alpha (ESRRA), were largely unaltered upon acute WCS exposure and slightly decreased upon chronic WCS exposure and cessation in differentiated ALI-PBEC cultures (Fig. 6). Interestingly though, in line with increased levels of PPRC1 as described above, fractionation of basal and luminal fractions revealed increased mRNA levels of *ESRRA* and *TFAM* in response to WCS (Fig. 6D). Variable, but minor, changes of the abundance of indices involved in mitochondrial biogenesis were observed in response to WCS (increases) and CSE (decreases) in undifferentiated S-PBEC cultures (Fig. S7).

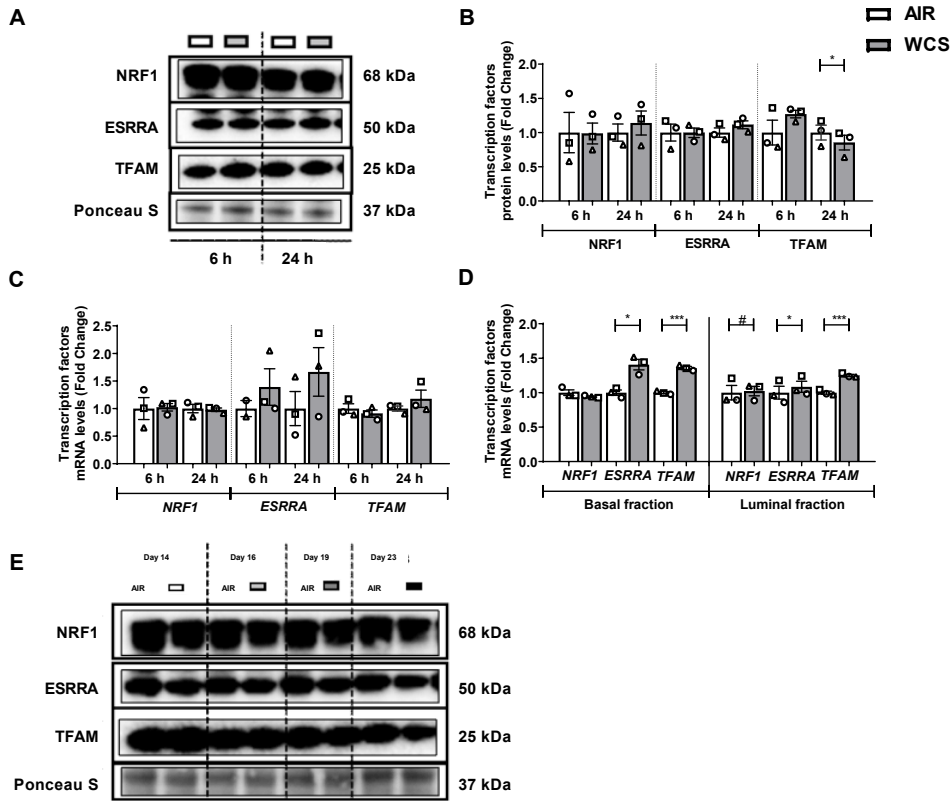

Continued to next page

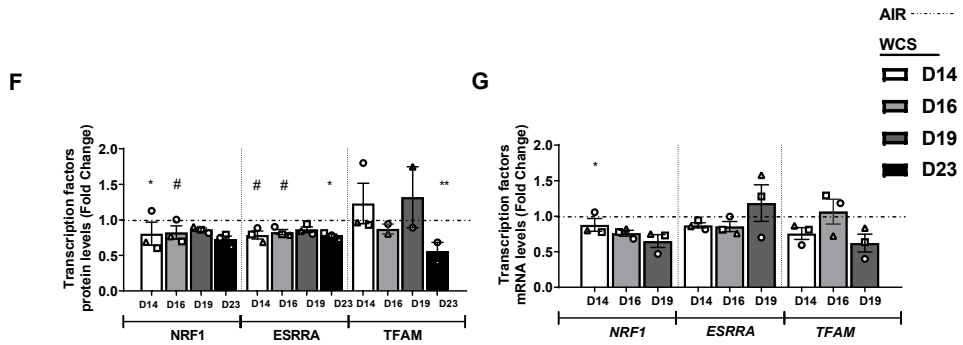

Figure 6. Alterations in the abundance of PPARGC1-coactivated transcription regulators in WCS-exposed ALI-PBEC. After 2-weeks of differentiation, ALI-PBEC were exposed to fresh air or WCS from one 3R4F cigarette (University of Kentucky, 2 mg) and whole cell lysates or basal and luminal cell fractions were harvested after respectively 6 h and 24 h or only 6 h post-exposure, respectively (n=3 donors/group). Protein **(A, B)** as well as mRNA levels **(C, D)** of PPARGC1-coactivated transcription regulators: NRF1, ESRRA, TFAM were analyzed in whole cell lysates or basal/luminal cell fractions post exposure. ALI-PBEC were 1x daily exposed to fresh air or WCS from one 3R4F cigarette (University of Kentucky, 2 mg) during differentiation for 14 days followed by a cessation period up to 10 days. Cells were harvested on Day 14 (24 h after the last exposure), 16, 19 and 23 (n=3 donors/group). Protein **(E, F)** and transcript abundance **(G)** of PPARGC1-coactivated transcription regulators are presented. Representative western blots are shown. Data are presented as mean fold change compared to control (air or WCS Day 14) ± SEM. Statistical significance is indicated as $^{\#}p<0.1$, $*p<0.05$ and $**p<0.01$ compared to control (air or WCS Day 14).

Collectively, these data show that expression of transcriptional co-activators involved in mitochondrial biogenesis were largely unaltered in whole cell lysates while increased abundance was observed in specific cell fractions of acute WCS-exposed ALI-PBEC and in basal cells of WCS-exposed S-PBEC. Moreover a different response was observed in the other *in vitro* CS exposure models. However, the observed increases, particular in PPRC1, but also alterations in abundance of some transcription factors associated with this co-activator molecules following CS exposure, may suggest a compensatory cellular response to induce mitochondrial biogenesis.

Changes in the regulation of mitochondrial fusion and fission in response to WCS exposure

Because of the observed changes in these mitochondrial quality control mechanisms in the different models and the fact that these processes require mitochondrial fusion and fission, we examined the impact of WCS exposure on key molecules involved in the regulation of mitochondrial dynamics. Acute WCS-treatment resulted in upregulation of mitochondrial fusion markers mitofusin (MFN) 1 (*MFN1*)

in ALI-PBEC (Figs S8A, B, C, D, E). However, CSE or WCS exposure had no pronounced impact on the regulation of fission or fusion markers in S-PBEC (Fig. S9). Also, no pronounced alterations were observed in the abundance of mitochondrial dynamic regulators upon chronic WCS exposure and the smoking cessation period (Figs S8F, G, H).

Disruption of the metabolic phenotype upon WCS exposure

We next investigated whether CS-induced changes in the regulation of mitochondrial biogenesis and mitophagy were accompanied by changes in mitochondrial content and mitochondrial metabolic pathways. To this end, we investigated effects of WCS exposure on the activity of critical metabolic enzymes and abundance of proteins involved in mitochondrial metabolic pathways.

Acute WCS exposure of differentiated ALI-PBEC cultures as well as CSE exposure of undifferentiated S-PBEC did not affect mitochondrial content as assessed by mitochondrial DNA copy number (Figs S10A and S11A). Also, protein and mRNA levels of nuclear-encoded and mitochondrial-encoded proteins and genes of electron-transport chain (ETC) subunits were unaltered after acute or chronic exposure of ALI-PBEC to WCS (Figs S10B, C, D, E, F, G, H). Some minor, but variable, alterations were found in transcript and protein abundance of analyzed subunits of ETC complexes in undifferentiated S-PBEC cultures exposed to CSE or WCS, respectively decreased *versus* increased abundance (Figs S11B, C, D). Although we did observe some slight alterations in the abundance of ETC subunits in the different models, in general, our data indicate no marked changes in indices of mitochondrial content in all models after acute or chronic exposure to CS.

We also examined the impact of CS exposure on the activity and abundance of constituents of the fatty acid β-oxidation and tricarboxylic acid cycle. Besides downregulated HADH enzyme activity in acute WCS-exposed ALI-PBEC, we also observed increased citrate synthase activity in CSE-treated S-PBEC (Figs S12A, E). Similar changes at mRNA level were found in the basal fraction of WCS-exposed ALI-PBEC, while conflicting but transient gene expression was found in S-PBEC CS models (Figs S12B, C, D, F).

Finally, we explored whether CS exposure may affect the metabolic program in PBEC. First, lactate production was measured in the basal medium of WCS-exposed ALI-PBEC. We observed an increase in L-lactate levels after acute and chronic WCS exposure of differentiated ALI-PBEC cultures compared to air control, which persisted after WCS cessation indicating a shift to a glycolytic metabolism (Figs 7A, F). In line with this, mRNA abundance of Hexokinase 2 (HK2), the enzyme responsible for the first step in glycolysis, was found to be elevated in acute and chronic WCS-exposed ALI-PBEC and in S-PBEC lysates (Figs 7E, H and S13E). Activity or expression levels of

other markers of glycolysis (PFK 1 enzyme activity and HK2 protein levels) that we measured showed no significant differences in response to acute or chronic WCS-exposed ALI-PBEC (Figs 7B, C, D, G). No significant differences were observed in L-lactate levels after acute WCS exposure in undifferentiated S-PBEC (Fig. S13A) or in activity of PFK 1 and abundance of HK2 in CSE-exposed S-PBEC (Figs S13B, C, D, E).

Collectively, these results demonstrate that CS exposure does not affect mitochondrial DNA copy number or the abundance of constituents of the ETC but do suggest a shift to a more glycolytic metabolism in fully differentiated PBEC cultures, but not in damaged epithelium.

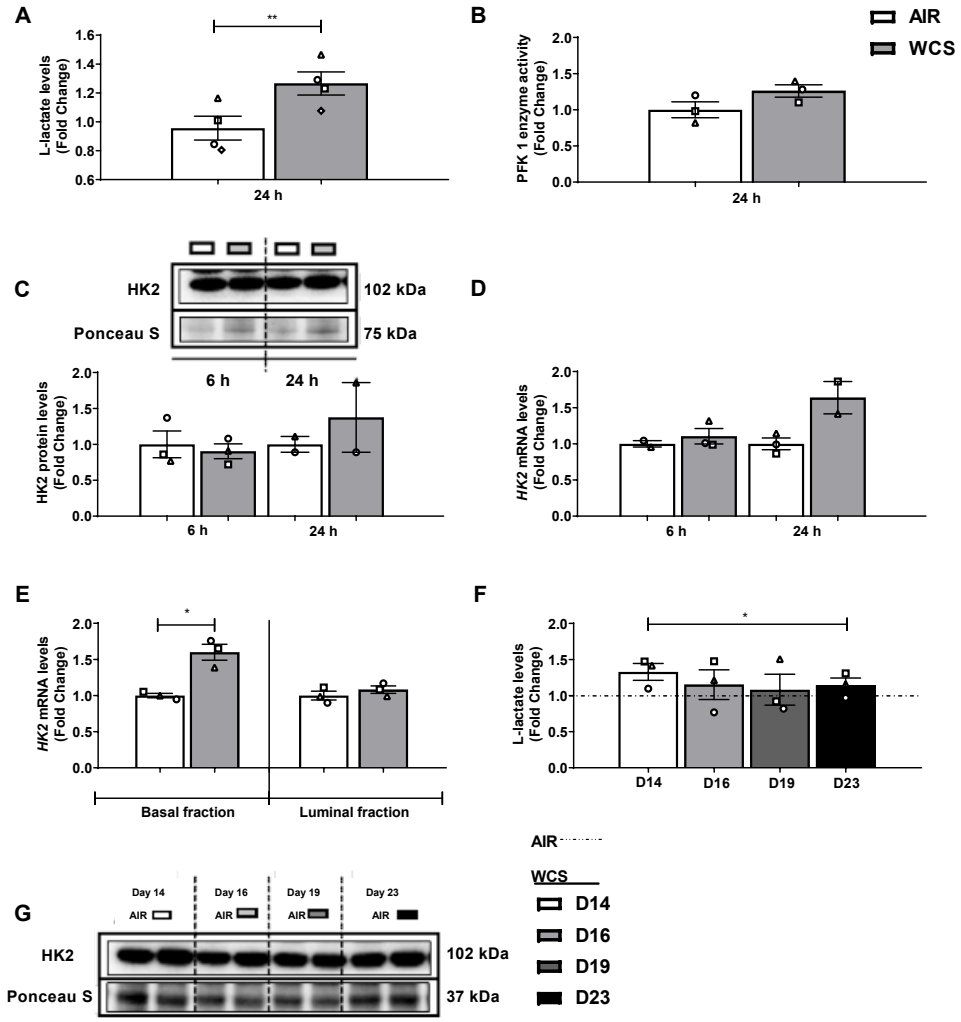

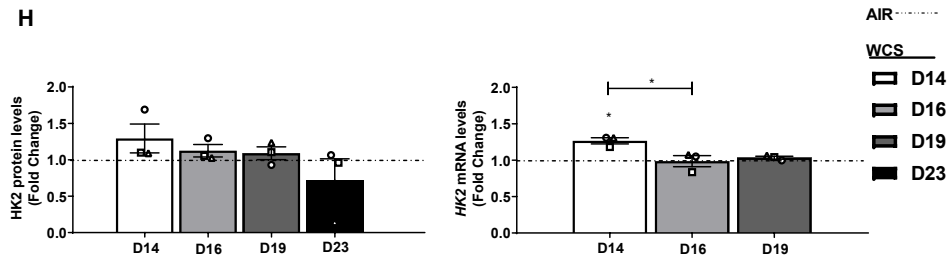

Figure 7. WCS-induced shift to anaerobic glycolysis in ALI-PBEC. After 2-weeks of differentiation, ALI-PBEC were exposed to fresh air or WCS from one 3R4F cigarette (University of Kentucky, 2 mg) and basal medium, whole cell lysates or basal and luminal cell fractions were harvested after respectively 6 h and 24 h or only 6 h post-exposure, respectively (n=3 donors/group). L-Lactate levels **(A)** in basal medium, PFK 1 activity **(B**), protein **(C)** and mRNA levels **(D, E)** of HK2 were analyzed in whole cell lysates or basal/luminal cell fractions post exposure. ALI-PBEC were 1x daily exposed to fresh air or WCS from one 3R4F cigarette (University of Kentucky, 2 mg) during differentiation for 14 days followed by a cessation period up to 10 days. Basal medium and cells were harvested on Day 14 (24 h after the last exposure), 16, 19 and 23 (n=3 donors/group). L-lactate levels **(F)**, protein **(G)** and transcript abundance **(H)** of HK2 are shown. Representative western blots are shown. Data are presented as mean fold change compared to control (air or WCS Day 14) ± SEM. Statistical significance is indicated as $^{\#}p<0.1$, $*p<0.05$ and $**p<0.01$ compared to control (air or WCS Day 14) .

Discussion

In our study, for the first time, we examined/compared the impact of acute WCS and CSE exposure on the molecular mechanisms regulating mitochondrial content and function in multiple PBEC models, ranging from undifferentiated cells that were exposed to CSE in a submerged culture to well-differentiated cultures exposed to WCS in an ALI system. In addition to studying acute effects of exposure on these regulatory processes, we also evaluated the persistence of effects following chronic WCS exposure during differentiation and potential recovery upon cessation of WCS exposure.

First and foremost, we observed a potent increase in the abundance of general autophagy proteins in differentiated cultures acutely exposed to WCS and demonstrated that these changes were localized to both basal and luminal cell fractions. Interestingly, these changes were largely absent in PBECs repeatedly exposed to WCS during differentiation. Indicative of a general autophagy response to acute smoke exposure, similar findings were observed in undifferentiated PBEC both in response to acute WCS and CSE exposure. Also, mitophagy-related protein and transcript abundance, specifically those involved in receptor-mediated mitophagy, increased in response to smoke exposure in several of our models. Increases in abundance of proteins involved in receptor-mediated mitophagy

were mainly observed in differentiated cultures, persisted after chronic exposure and remained elevated for the duration of the smoke cessation protocol. Analysis of markers of mitochondrial content and mitochondrial dynamics revealed no pronounced changes in response to WCS or CSE in any of our models. We did observe however that differentiated PBEC cultures acutely exposed to WCS displayed minor changes in the abundance of proteins involved in mitochondrial biogenesis, as well as a metabolic shift towards more glycolytic phenotype. These findings are summarized in Table 2. As depicted in the table, we did observe several differences in the response of our different PBEC cultures to WCS or CSE. This highlights the importance of tailoring the *in vitro* model to the research question with regard to studying the impact of (chemical) exposure-induced mitochondrial abnormalities in the context of respiratory disease.

Table 2. Summary of changes in the molecular regulation of mitochondrial metabolism in four PBEC models of CS exposure

		ALI-PBEC			S-PBEC	
Processes involved in mitochondrial quality control		**acute WCS**	**chronic WCS**	**chronic WCS cessation**	**acute WCS**	**CSE treatment**
Autophagy		↑↑	↑ / ↓	=	↑↑	↑↑
Mitophagy	Receptor-mediated	↑	↑	=	=	↑
	Ubiquitin-mediated	↓	=	=	=	↓
Mitochondrial biogenesis	PPARGC1 co-activators	↑	↓	=	↑	↓
	PPARGC1 co-activated transcription factors	↑	↓	=	↑	↓
Glycolytic metabolism		↑	↑	↓	↑	=
Mitochondrial dynamics	Fission	=	=	=	↑	=
	Fusion	↑	=	=	↑	=
Mitochondrial content		=	=	=	↑	↑ / ↓

Summary of the protein and transcript expression of regulators involved in mitochondrial metabolism (e.g., biogenesis versus mitophagy) analyzed by western blot and real time qPCR in four PBEC models of exposure to WCS or CSE. These included (1) differentiated ALI-PBEC acutely-exposed to WCS (including whole cell lysates and separated basal and luminal fractions), (2) ALI-PBEC chronically-exposed (during differentiation) to WCS followed by smoking cessation, (3) undifferentiated S-PBEC acutely-exposed to WCS, and (4) undifferentiated S-PBEC treated with CSE (submerged). The effect of acute CS exposure in the PBEC models (WCS and CSE, S-PBEC and ALI-PBEC) was assessed by comparison to fresh air or 0% CSE, except in the chronic WCS cessation model, in which we also compared WCS exposure at Day 16, 19, 23 to 24 h post chronic WCS exposure (WCS Day 14). Arrows point to the direction of change; one arrow means fold change <2 and two arrows indicates a fold change >2 of treatment versus control (air, 0 % CSE or WCS Day 14). ↓/↑ indicates a differential response of various markers. = indicates no change in response to smoke exposure compared to

control. Only significant differences are indicated. ALI-PBEC, undifferentiated PBEC cultured at the air-liquid interface to induce differentiation; CS, cigarette smoke; CSE, CS extract; PBEC, primary bronchial epithelial cells; WCS, whole CS; S-PBEC, PBEC cultured in submerged conditions.

Summary of the protein and transcript abundance of regulators involved in mitochondrial metabolism (e.g., biogenesis *versus* mitophagy) analyzed by western blot and real time qPCR in four PBEC models of exposure to WCS or CSE. These included respectively A) differentiated ALI-PBEC acutely-exposed to WCS (including whole cell lysates and separated basal and luminal fractions), B) ALI-PBEC chronically-exposed (during differentiation) to WCS followed by smoking cessation, C) undifferentiated S-PBEC acutely-exposed to WCS, and D) undifferentiated S-PBEC treated with CSE (submerged). The effect of acute CS exposure in the PBEC models (WCS and CSE, S-PBEC and ALI-PBEC) was assessed by comparison to fresh air or 0% CSE, except in the chronic WCS cessation model in which we also compared WCS exposure at Day 16, 19, 23 to 24 h post chronic WCS exposure (WCS Day 14). Arrows point to the direction of change; one arrow means fold change <2 and two arrows indicates a fold change >2 of treatment *versus* control (air, 0 % CSE or WCS Day 14). ↓/↑ indicates a differential response of various markers. = indicates no change in response to smoke exposure compared to control. Only significant differences are indicated.

We observed increases in the abundance of both protein and transcript levels of key constituents of autophagy in luminal as well as basal fractions of differentiated cultures as well as in whole cell lysates of non-differentiated cultures. Collectively, this implies that this is a robust response of different bronchial epithelial cell types to CS constituents and is reflected in both intact as well as damaged epithelium (both of which are present in the airways of COPD patients). These data are in line with previous findings in CS(E)-treated human airway epithelial cells (24, 25, 29, 30, 52), in lung homogenates of (a majority of ex-smoking) COPD patients (24, 53) and in CS-exposed mice (9, 24, 53). Furthermore, they provide further support for the hypothesis that imbalanced autophagy, and in particular excessive autophagy induction, has been implicated in the pathogenesis of COPD by resulting in programmed cell death of epithelial cells and subsequent development of pulmonary emphysema (54).

Induction of autophagy likely results from (sub)cellular damage by oxidative components present in CS (54, 55). In line with this notion and with previous studies (25), we did observe modulation of cellular anti-oxidant systems in response to WCS in our models. Although a robust induction of autophagy markers was observed in our acute exposure models, chronic exposure to WCS resulted in a decreased ratio of LC3BII/I in differentiating PBECs which recovered during smoke cessation. In line with this observation, a recent study showed low amounts of LC3B positive cells in cultured PBEC from severe COPD patients, possibly associated with a decreased

number of club cells but independent of cellular stress (56). As a persistent loss of the club cell marker SCGB1A1 has been previously demonstrated in our chronic WCS model (36), the differential effects of chronic versus acute WCS exposure on autophagy markers and recovery upon cessation could be potentially explained by both oxidative stress and aberrant differentiation and/or loss of club cells in response to chronic smoke exposure (36). These speculations on the relationship between autophagy and aberrant epithelial cell differentiation are supported by observations showing that autophagy inhibits ciliated cell differentiation (57) and regulates mucin production by goblet cells in the airway epithelium (58). Although blocking induction of autophagy (e.g. after smoke exposure) may improve epithelial function (30, 59), autophagy may also serve a protective function by enabling adequate restoration of airway epithelial function after an insult (60, 61). Collectively these studies indicate that CS-induced increases in autophagy contributes to aberrant epithelial differentiation upon smoke exposure.

Mitophagy is a form of targeted autophagy that can contribute to the clearance of damaged mitochondria that have been found following exposure to CS in multiple human and mice airway epithelial cell types in lung tissue as well as in PBEC cultures from COPD patients (25, 26, 62). In our study, we found an increased abundance of specific proteins involved in receptor-mediated mitophagy in response to both acute and chronic stimulation with WCS or CSE in different cell populations which persisted during the cessation period. To the best of our knowledge, only a few previous studies investigated the impact of CS on the regulation of receptor-mediated mitophagy in airway epithelial cells. These studies reported an increase of receptor-mediated mitophagy proteins in response to smoke exposure both *in vivo* and *in vitro* (30, 59).

Interestingly, it has been shown that cellular hypoxia-related signaling [i.e. hypoxia-inducible factor (HIF1α)] is activated by smoke exposure in these airway epithelial cell models (63-65). Moreover, it is known that hypoxia activates receptor-mediated mitophagy in various cell types (66-71) as HIF1α has been recognized as upstream regulator of BNIP3(L) (67, 72, 73). Therefore, it can be speculated that CS-induced hypoxia partly contributes to the observed CS-induced elevated receptor-mediated mitophagy. Moreover, indicative of a contribution of CS-induced activation of receptor-mediated mitophagy to COPD pathology, one study reported amelioration of COPD-like features in mice with genetically blocked receptor-mediated mitophagy (59). In contrast to the observed robust changes in receptor-mediated mitophagy in response to CS in our models, changes in mediators of ubiquitin-mediated mitophagy were less pronounced. In general, we observed that PINK1 protein and transcript levels tended to be increased in response to acute CS exposure while PRKN levels decreased. This is in line with literature as CS-induced increases in PINK1 levels and decreased PRKN abundance have been described in several *in vitro/vivo* (airway) models (9, 16, 25, 26, 31, 32) and in peripheral lung tissue and bronchial epithelial

cells of (ex-smoking) COPD patients (9, 11, 25, 26). In contrast to these findings however, other studies reported no changes or even increases in the abundance of these constituents of ubiquitin-mitophagy in response to CS in various *in vitro* and *in vivo* models of exposure of cells of the airways to CS as well as in lungs of COPD patients (9-11, 16, 26, 62).

In general, whether or not mitophagy serves a protective or detrimental role in CS-induced COPD development remains controversial. Indeed, previous studies have reported that knock-down/out of PINK1 or PRKN (9, 25, 31, 74) as well as overexpression of PRKN (25, 26, 74) protected against CSE-induced mitophagy or mitochondrial dysfunction in *in vitro* or *in vivo* models, highlighting the complexity of regulation of mitophagy. Seemingly discrepant findings regarding CS-induced mitophagy in literature may stem from differences in dose and time of exposure of cells to CS constituents (mild *versus* severe CS stress) or from the dynamic (flux) nature of mitophagy. The fact that in our study the induction of receptor-mediated mitophagy was more pronounced than ubiquitin-mediated mitophagy and that *in vivo* models of smoke exposure (or COPD) often describe activation of this PINK1/PRKN pathway (9, 25, 26), may be related to the fact that our *in vitro* models lack the inflammatory cells which are present in *in vivo* in smoke-induced COPD. Important to consider in this regard is that inflammation is known to be linked to mitochondrial dysfunction (75, 76) and inflammatory mediators have been shown to induce the PINK1/PRKN pathway in epithelial cells (77). Further studies focusing on the molecular mechanisms of these pathway-specific regulation of mitophagy in epithelial cell types need to be conducted.

Besides clearance of damaged mitochondria by mitophagy, mitochondrial biogenesis is crucial in maintaining mitochondrial homeostasis. Interestingly, we observed that some proteins involved in mitochondrial biogenesis were increased in response to acute WCS exposure, while both CSE and chronic WCS exposure resulted in decreased abundance of these molecules. In line with our findings, previous studies also observed differential effects of short-term or long-term CS exposure on mitochondrial biogenesis. For example, whereas short-term CS treatment of cultured human bronchial epithelial cells increased transcript abundance of PPARGC1A, long-term CS exposure did not affect mitochondrial biogenesis (11). Similar findings were also observed in lung tissue from COPD patients in different disease stages ranging from mild to severe COPD (11, 78, 79). Collectively, increased mitochondrial biogenesis in acute WCS models might indicate an adaptive cellular response to protect against mitochondrial damage by inducing mitochondrial biogenesis, while decreased mitochondrial biogenesis in chronic WCS model might reflect an inability to compensate for these changes.

We did not find pronounced differences in the abundance of fusion and fission indices after CS exposure in our models. Previous studies have found that short or

long-term CSE exposure can induce changes in proteins regulating mitochondrial dynamics with effects on mitochondrial morphology (9, 62). These effects were found to range from swollen, fragmented organelles to mitochondrial hyperfusion (9, 10, 17, 28, 31, 32, 62, 80), and the variability in CSE preparation (including type of cigarette used, concentration and generation of CSE) may explain the conflicting findings in *in vitro* studies. As we did not assess mitochondrial morphology in our study, no solid conclusions can be drawn about the impact of CS exposure in our models.

mtDNA damage and disturbed mitochondrial metabolism, including impaired respiratory capacity and abundance/ activity of subunits of ETC complexes, have been described in multiple *in vitro* or *in vivo* (airway) models in response to CS(E) (3, 6, 9-11, 16, 29). Importantly, several studies demonstrated that CS-induced mitochondrial dysfunction is causally implicated in CS-induced disruption of the functionality of the bronchial epithelium (81) as well as in the development of COPD (3). In our study, we did not observe large changes in mtDNA copy number or the abundance of oxidative phosphorylation complexes. As mtDNA copies vary per cell type and only selective subunits of various complexes were analyzed, additional studies are required. We cannot exclude the possibility that increased mitochondrial biogenesis may have compensated for potential loss of mitochondria in our models.

In line with prior evidence reporting CS-induced metabolic reprogramming of airway epithelial cells (13, 82), mouse lungs (83) or in COPD (84-87), we observed increased lactate production in our models in response to WCS which persisted during chronic WCS exposure and cessation. Although we did not assess mitochondrial function by respirometry or complex activity analysis, and therefore cannot decisively conclude about the impact of CS on mitochondrial function, the fact that lactate increases does suggests abnormalities in mitochondrial oxidative metabolism. Moreover, metabolic reprogramming is suggested to be a driver of CS-induced inflammatory lung diseases (88). Additionally, it has been reported that lactate produced as a result of smoke-induced deregulation of cellular metabolism directly binds to transmembrane domain of mitochondrial antiviral-signalling protein (MAVS) and thus prevents MAVS aggregation, resulting in an inhibition of type I interferon production, impaired anti-viral response and enhanced viral replication (89). Since it is well established that cigarette smoking increases susceptibility to viral infections (90), which was replicated in in vitro epithelial culture models (including our WCS for rhinovirus infection) (91-93), these data suggest that our observation of increased lactate production upon WCS exposure may partly explain the impact of cigarette smoke exposure on epithelial susceptibility to virus infections.

To better understand the impact of CS on mitochondrial quality control processes in simple and advanced *in vitro* PBEC models, we included four models which cover a variation in type and duration of CS exposure, epithelial cell types and read-out

parameters. Obviously, the different exposure scenarios influence the results since during WCS (that includes volatiles) exposure, the cells are directly and shortly exposed, while via incubating with CSE (only dissolved, aqueous components) in the medium the contact time with CS components will be longer. While a similar response in these two exposure models can be explained by the impact of aqueous CS components (present in both CS and CSE), a conflicting response could be due to the continuous exposure of CSE (e.g. receptor-mediated mitophagy) or additional volatiles present in WCS. However, in general the non-standardized methods of WCS or CSE preparation, e.g. variability in type of cigarette, concentration determination and generation (often in-house developed systems), make it difficult to compare results of different smoke exposure studies.

The strength of our study is the investigation, for the first time, of a comprehensive panel of markers involved in the regulation of mitochondrial metabolism in various relevant CS exposure *in vitro* primary human airway epithelial cell models. The novelty of our findings is multifaceted (Fig. 8). First, the exclusive use of human PBEC (differentiated or undifferentiated) from multiple donors (Table 1) to assess CS-induced changes in mitochondrial homeostasis is a considered a strength as most studies investigating this topic deployed cell lines or rodent exposure studies. Second, we exposed fully differentiated cultures of PBEC directly and shortly to WCS (gas and particulate phase, short-and long-lived CS constituents) in an ALI system which adequately mimics the real-life exposure. Reports using this model and exposure system are very limited (likely due to the complexity of the culture- and exposure system), and most studies using primary cells employed undifferentiated submerged cultures that were exposed to CSE rather than WCS. Moreover, the combination of these various models (CSE and WCS, undifferentiated S-PBEC and differentiated ALI-PBEC) adds important novelty and insight to the field. Third, we analyzed changes in the regulation of mitochondrial homeostasis in luminal or basal cell fractions of the differentiated pseudostratified epithelium, which has not previously been reported. Fourth, whereas studies usually examined a selection of markers related to on or two mitochondrial processes, we here investigated for the first time a comprehensive panel of markers involved in all important processes associated with the regulation of mitochondrial metabolism in our *in vitro* CS exposure models of PBEC. Lastly, studying this subset of molecules involved in mitochondrial metabolism in four relevant CS exposure *in vitro* PBEC cell models allows important comparisons not only within our four different models but also with data present in literature. The relevance of our findings is enhanced by using PBEC derived from multiple donors (different in various experiments), cultured in both (un)differentiated submerged and ALI conditions and comparison of different type and duration of CS exposure.

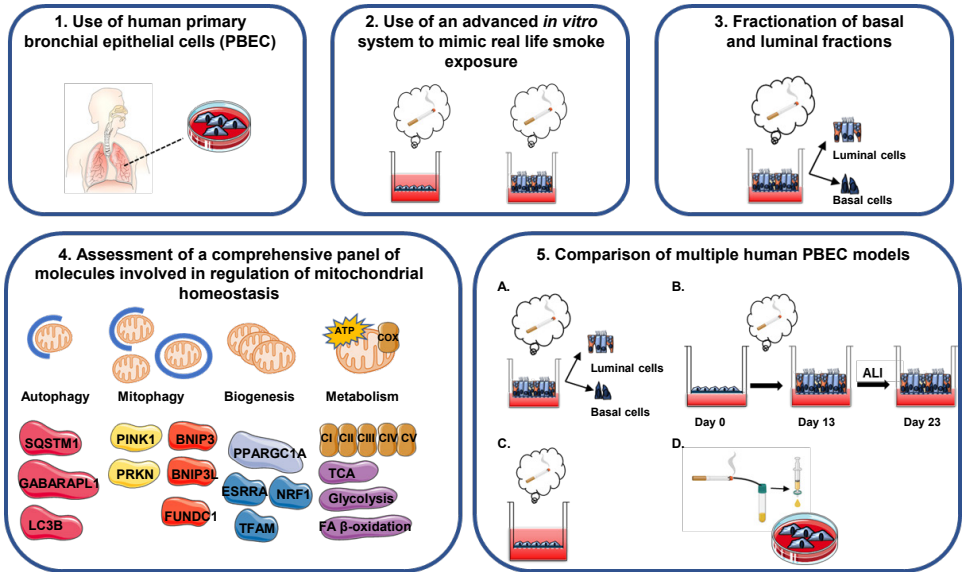

Figure 8. Overview of experimental approach. Schematic representation of the novelty and strengths of the study. 1. Use of human primary bronchial epithelial cells (PBEC): human PBEC (differentiated or undifferentiated) from multiple donors (non-COPD patients) were used to assess CS-induced changes in mitochondrial homeostasis. 2. Use of an advanced *in vitro* system to mimic real-life smoke exposure: fully differentiated cultures of PBEC were directly and shortly exposed to WCS in an air-liquid interface (ALI) system. 3. Fractionation of basal and luminal fractions: changes in the regulation of mitochondrial homeostasis in basal and luminal fractions of WCS-exposed differentiated PBEC were investigated. 4. Assessment of a comprehensive panel of molecules involved in regulation of mitochondrial homeostasis: a comprehensive panel of markers involved in all important processes associated with the regulation of mitochondrial metabolism were investigated in the CS exposure *in vitro* PBEC models. 5. Comparison of multiple human PBEC models (A-D): studying of these subset of molecules involved in mitochondrial metabolism in four relevant CS exposure *in vitro* PBEC models allows important comparisons not only within our four different models but also with data present in literature.

The differentiated epithelial cultures used in the present study mimic an intact pseudostratified epithelium relevant to study responses to inhalation toxicants of an intact epithelial layer, while the undifferentiated PBEC model represents a basal cell-like structure relevant to study responses of a partly denuded epithelial layer. Moreover, chronic WCS exposure of a differentiating epithelial layer followed by cessation of exposure, provided the opportunity to investigate repair. Strikingly, we observed abnormalities at the level of mitochondrial quality control mechanisms in all models, suggestive of a role for CS-induced mitochondrial dysfunction in different areas of the bronchial epithelium relevant for COPD. Differential responses that we observed highlight the importance of making considered choices for (un) differentiated cell models, type of CS exposure and duration of smoking in future

respiratory inhalation (toxicology) studies tailored to the research question.

Inevitably, our study obviously also has several limitations. First, a limited number of donors was investigated. Second, although our short-term CS exposure models may mimic changes in airway epithelial cells from chronic smokers, including autophagy, differences between molecular changes in response to acute versus chronic smoke exposure or with changes in lung homogenates from COPD patients were observed, as illustrated by the findings on mitochondrial biogenesis or ubiquitin-mediated mitophagy. Furthermore, as mitochondrial biogenesis, mitophagy, and mitochondrial dynamics are fluxes, the fact our analyses represent a snapshot of these processes is a limitation. Because our current research aimed to compare CS-induced alterations in the molecular mechanisms underlying mitochondrial function among four different models, we did not focus on implications of CS-induced molecular changes on functional changes in epithelial homeostasis, including repair, differentiation and remodelling as well as for example epithelial barrier function, cilia beating, antiviral responses and mucus production. However, the impact of acute and chronic cigarette smoke exposure on the abovementioned aspects of epithelial function has previously been reported by us in the models used in the present study (36, 41, 93-96) and other research groups (97-101). In addition, direct associations between mitochondrial dysfunction, deregulated autophagy and lactate production and epithelial function have been reported previously (3, 30, 57-60, 81). Whereas we only separated luminal and basal cells in our differentiated ALI-PBEC model that includes several epithelial cell types, additional research should evaluate the impact of CS exposure in individual luminal cell types, as well as in alveolar cells as those are also markedly affected in COPD. Furthermore, additional experiments need to be conducted considering effects of CS exposure on mitochondrial quality control processes using advanced state-of-the-art *in vitro* models and more realistic WCS exposure methods including varying puff-topography regimes reflecting human smoking behavior.

Our model is limited to (differentiated) epithelial cells and did not include other cell types such as immune cells. However, our observations are supported by findings in lung tissue of COPD patients showing mitochondrial alterations and increased autophagy. Moreover, other studies reported similar molecular changes of mitochondrial metabolism in *in vivo* smoke exposure models and have demonstrated that these are not only associated with but also causally related to functional and structural abnormalities in the bronchial and alveolar compartment reminiscent of COPD lung/airway pathology (3, 9, 24). Future studies using more complex models such as co-culture (93), lung on chips (94) or ex vivo precision-cut lung slices (95) to investigate the individual molecular changes at global, single-cell and tissue levels have the potential to overcome part of these limitations. We have previously reported the feasibility of such an approach by showing that macrophages support epithelial repair in our WCS exposure model using cocultures of epithelial cells and

monocyte-derived macrophages (96). Moreover, although our study has a targeted approach, future studies could focus on a more 'global' multi-omics approach to investigate the impact of smoke exposure on mitochondrial metabolism. Other studies have used such approaches; for example, metabolomics has been used to elucidate the role of smoke-induced metabolic reprogramming in the pathogenesis of lung diseases (102), lipidomics was used by us to show that polyunsaturated fatty acid metabolism is affected by exposure of ALI-PBEC to WCS and altered in sputum from COPD patients compared to controls (103), and transcriptomics analysis of CS-exposed ALI cultures reported critical molecular pathways involved in aberrant tissue remodeling and lung disease-associated pathways (104). Interestingly, a multi-omics approach has also been applied in repeated CS-exposed co-cultures of bronchial tissue, revealing alterations in molecular pathways involved in airway diseases (105). However, these studies did not compare the different culture or exposure models used in the present study.

In conclusion, in this study, differences were observed in the regulation of mitochondrial metabolic processes in the four investigated models reflecting damaged, intact, differentiating or repairing airway epithelium, and multiple CS exposure regimes. The results highlight the robust model-independent impact of CS exposure on the abundance of key molecules involved in autophagy and receptor-mediated mitophagy. These alterations were, at least in part although less pronounced, recapitulated after chronic exposure of differentiating epithelial cells to CS. Differences observed in the regulation of mitochondrial metabolic processes, such as mitochondrial biogenesis, in the investigated models, reflecting various cell types of the epithelium and CS exposure regimes, supports the importance of tailoring the experimental model to the research question.

Acknowledgements

The authors would like to thank Mieke Dentener and Nico Kloosterboer of the Primary Lung Culture Facility (PLUC; Maastricht University Medical Center+) for providing donor cells, advice, and protocols.

Competing interests

The authors have declared that no competing interests exist.

Funding

This research is supported by the Netherlands Food and Consumer Product Safety Authority (NVWA) and by a fellowship from the China Scholarship Council.

References

1. Celli BR, Wedzicha JA. Update on Clinical Aspects of Chronic Obstructive Pulmonary Disease. N Engl J Med. 2019;381(13):1257-66.
2. WHO. The top 10 causes of death: World Health Organization; 2020 [Available from: https://www.who.int/news-room/fact-sheets/detail/the-top-10-causes-of-death.
3. Cloonan SM, Glass K, Laucho-Contreras ME, Bhashyam AR, Cervo M, Pabon MA, et al. Mitochondrial iron chelation ameliorates cigarette smoke-induced bronchitis and emphysema in mice. Nat Med. 2016;22(2):163-74.
4. Cloonan SM, Choi AM. Mitochondria in lung disease. J Clin Invest. 2016;126(3):809-20.
5. Prakash YS, Pabelick CM, Sieck GC. Mitochondrial Dysfunction in Airway Disease. Chest. 2017;152(3):618-26.
6. Aghapour M, Remels AHV, Pouwels SD, Bruder D, Hiemstra PS, Cloonan SM, et al. Mitochondria: at the crossroads of regulating lung epithelial cell function in chronic obstructive pulmonary disease. Am J Physiol Lung Cell Mol Physiol. 2020;318(1):L149-l64.
7. Pan S, Conaway S, Jr., Deshpande DA. Mitochondrial regulation of airway smooth muscle functions in health and pulmonary diseases. Arch Biochem Biophys. 2019;663:109-19.
8. Hiemstra PS, van der Does AM. Reprogramming of cellular metabolism: driver for airway remodelling in COPD? Eur Respir J. 2017;50(5).
9. Mizumura K, Cloonan SM, Nakahira K, Bhashyam AR, Cervo M, Kitada T, et al. Mitophagy-dependent necroptosis contributes to the pathogenesis of COPD. J Clin Invest. 2014;124(9):3987-4003.
10. Sundar IK, Maremanda KP, Rahman I. Mitochondrial dysfunction is associated with Miro1 reduction in lung epithelial cells by cigarette smoke. Toxicol Lett. 2019;317:92-101.
11. Hoffmann RF, Zarrintan S, Brandenburg SM, Kol A, de Bruin HG, Jafari S, et al. Prolonged cigarette smoke exposure alters mitochondrial structure and function in airway epithelial cells. Respir Res. 2013;14:97.
12. Malinska D, Szymanski J, Patalas-Krawczyk P, Michalska B, Wojtala A, Prill M, et al. Assessment of mitochondrial function following short- and long-term exposure of human bronchial epithelial cells to total particulate matter from a candidate modified-risk tobacco product and reference cigarettes. Food Chem Toxicol. 2018;115:1-12.
13. Agarwal AR, Yin F, Cadenas E. Short-term cigarette smoke exposure leads to metabolic alterations in lung alveolar cells. Am J Respir Cell Mol Biol. 2014;51(2):284-93.
14. Valdivieso Á G, Dugour AV, Sotomayor V, Clauzure M, Figueroa JM, Santa-Coloma TA. N-acetyl cysteine reverts the proinflammatory state induced by cigarette smoke extract in lung Calu-3 cells. Redox Biol. 2018;16:294-302.
15. van der Toorn M, Rezayat D, Kauffman HF, Bakker SJ, Gans RO, Koëter GH, et al. Lipid-soluble components in cigarette smoke induce mitochondrial production of reactive oxygen species in lung epithelial cells. Am J Physiol Lung Cell Mol Physiol. 2009;297(1):L109-14.
16. Wu K, Luan G, Xu Y, Shen S, Qian S, Zhu Z, et al. Cigarette smoke extract increases mitochondrial membrane permeability through activation of adenine nucleotide translocator (ANT) in lung epithelial cells. Biochem Biophys Res Commun. 2020;525(3):733-9.
17. Hara H, Araya J, Ito S, Kobayashi K, Takasaka N, Yoshii Y, et al. Mitochondrial fragmentation in cigarette smoke-induced bronchial epithelial cell senescence. Am J Physiol Lung Cell Mol Physiol. 2013;305(10):L737-46.
18. Jornayvaz FR, Shulman GI. Regulation of mitochondrial biogenesis. Essays Biochem.

2010;47:69-84.
19. Lin J, Handschin C, Spiegelman BM. Metabolic control through the PGC-1 family of transcription coactivators. Cell Metab. 2005;1(6):361-70.
20. Scarpulla RC. Metabolic control of mitochondrial biogenesis through the PGC-1 family regulatory network. Biochim Biophys Acta. 2011;1813(7):1269-78.
21. Gomes LC, Scorrano L. Mitochondrial morphology in mitophagy and macroautophagy. Biochim Biophys Acta. 2013;1833(1):205-12.
22. Fritsch LE, Moore ME, Sarraf SA, Pickrell AM. Ubiquitin and Receptor-Dependent Mitophagy Pathways and Their Implication in Neurodegeneration. J Mol Biol. 2020;432(8):2510-24.
23. Hikichi M, Mizumura K, Maruoka S, Gon Y. Pathogenesis of chronic obstructive pulmonary disease (COPD) induced by cigarette smoke. J Thorac Dis. 2019;11(Suppl 17):S2129-S40.
24. Chen ZH, Kim HP, Sciurba FC, Lee SJ, Feghali-Bostwick C, Stolz DB, et al. Egr-1 regulates autophagy in cigarette smoke-induced chronic obstructive pulmonary disease. PLoS One. 2008;3(10):e3316.
25. Ito S, Araya J, Kurita Y, Kobayashi K, Takasaka N, Yoshida M, et al. PARK2-mediated mitophagy is involved in regulation of HBEC senescence in COPD pathogenesis. Autophagy. 2015;11(3):547-59.
26. Ahmad T, Sundar IK, Lerner CA, Gerloff J, Tormos AM, Yao H, et al. Impaired mitophagy leads to cigarette smoke stress-induced cellular senescence: implications for chronic obstructive pulmonary disease. Faseb j. 2015;29(7):2912-29.
27. Mizumura K, Justice MJ, Schweitzer KS, Krishnan S, Bronova I, Berdyshev EV, et al. Sphingolipid regulation of lung epithelial cell mitophagy and necroptosis during cigarette smoke exposure. Faseb j. 2018;32(4):1880-90.
28. Song C, Luo B, Gong L. Resveratrol reduces the apoptosis induced by cigarette smoke extract by upregulating MFN2. PLoS One. 2017;12(4):e0175009.
29. Park EJ, Park YJ, Lee SJ, Lee K, Yoon C. Whole cigarette smoke condensates induce ferroptosis in human bronchial epithelial cells. Toxicol Lett. 2019;303:55-66.
30. Zhang M, Shi R, Zhang Y, Shan H, Zhang Q, Yang X, et al. Nix/BNIP3L-dependent mitophagy accounts for airway epithelial cell injury induced by cigarette smoke. J Cell Physiol. 2019;234(8):14210-20.
31. Kyung SY, Kim YJ, Son ES, Jeong SH, Park JW. The Phosphodiesterase 4 Inhibitor Roflumilast Protects against Cigarette Smoke Extract-Induced Mitophagy-Dependent Cell Death in Epithelial Cells. Tuberc Respir Dis. 2018;81(2):138-47.
32. Son ES, Kim SH, Ryter SW, Yeo EJ, Kyung SY, Kim YJ, et al. Quercetogetin protects against cigarette smoke extract-induced apoptosis in epithelial cells by inhibiting mitophagy. Toxicol In Vitro. 2018;48:170-8.
33. Hiemstra PS, Grootaers G, van der Does AM, Krul CAM, Kooter IM. Human lung epithelial cell cultures for analysis of inhaled toxicants: Lessons learned and future directions. Toxicol In Vitro. 2018;47:137-46.
34. Mertens TC, Karmouty-Quintana H, Taube C, Hiemstra PS. Use of airway epithelial cell culture to unravel the pathogenesis and study treatment in obstructive airway diseases. Pulm Pharmacol Ther. 2017;45:101-13.
35. Boei J, Vermeulen S, Klein B, Hiemstra PS, Verhoosel RM, Jennen DGJ, et al. Xenobiotic metabolism in differentiated human bronchial epithelial cells. Arch Toxicol. 2017;91(5):2093-105.
36. Amatngalim GD, Schrumpf JA, Dishchekenian F, Mertens TCJ, Ninaber DK, van der Linden

AC, et al. Aberrant epithelial differentiation by cigarette smoke dysregulates respiratory host defence. Eur Respir J. 2018;51(4):1701009.
37. Wang Y, Xu J, Meng Y, Adcock IM, Yao X. Role of inflammatory cells in airway remodeling in COPD. Int J Chron Obstruct Pulmon Dis. 2018;13:3341-8.
38. Rutgers SR, Postma DS, ten Hacken NH, Kauffman HF, van Der Mark TW, Koeter GH, et al. Ongoing airway inflammation in patients with COPD who Do not currently smoke. Chest. 2000;117(5 Suppl 1):262s.
39. Hodge S, Hodge G, Holmes M, Reynolds PN. Increased airway epithelial and T-cell apoptosis in COPD remains despite smoking cessation. European Respiratory Journal. 2005;25(3):447-54.
40. Schrumpf JA, Ninaber DK, van der Does AM, Hiemstra PS. TGF-β1 Impairs Vitamin D-Induced and Constitutive Airway Epithelial Host Defense Mechanisms. J Innate Immun. 2020;12(1):74-89.
41. Amatngalim GD, van Wijck Y, de Mooij-Eijk Y, Verhoosel RM, Harder J, Lekkerkerker AN, et al. Basal cells contribute to innate immunity of the airway epithelium through production of the antimicrobial protein RNase 7. J Immunol. 2015;194(7):3340-50.
42. van Wetering S, Zuyderduyn S, Ninaber DK, van Sterkenburg MAJA, Rabe KF, Hiemstra PS. Epithelial differentiation is a determinant in the production of eotaxin-2 and -3 by bronchial epithelial cells in response to IL-4 and IL-13. Molecular Immunology. 2007;44(5):803-11.
43. van Wetering S, van der Linden AC, van Sterkenburg MA, de Boer WI, Kuijpers AL, Schalkwijk J, et al. Regulation of SLPI and elafin release from bronchial epithelial cells by neutrophil defensins. Am J Physiol Lung Cell Mol Physiol. 2000;278(1):L51-8.
44. Carp H, Janoff A. Possible mechanisms of emphysema in smokers. In vitro suppression of serum elastase-inhibitory capacity by fresh cigarette smoke and its prevention by antioxidants. Am Rev Respir Dis. 1978;118(3):617-21.
45. Wang Y, Ninaber DK, van Schadewijk A, Hiemstra PS. Tiotropium and Fluticasone Inhibit Rhinovirus-Induced Mucin Production via Multiple Mechanisms in Differentiated Airway Epithelial Cells. Front Cell Infect Microbiol. 2020;10:278.
46. Amatngalim GD, Schrumpf JA, Dishchekenian F, Mertens TCJ, Ninaber DK, van der Linden AC, et al. Aberrant epithelial differentiation by cigarette smoke dysregulates respiratory host defence. Eur Respir J. 2018;51(4).
47. Shepherd D, Garland P. The kinetic properties of citrate synthase from rat liver mitochondria. Biochemical Journal. 1969;114(3):597-610.
48. Bergmeyer H, Gawehn K, Grassl M. 3-Hydroxyacyl-CoA dehydrogenase. Methods of enzymatic analysis. 1974;1:474.
49. Ling K, Paetkau V, Marcus F, Lardy HA. [77a] Phosphofructokinase: I. Skeletal Muscle. Methods in enzymology. 9: Elsevier; 1966. p. 425-9.
50. Yun HR, Jo YH, Kim J, Shin Y, Kim SS, Choi TG. Roles of Autophagy in Oxidative Stress. Int J Mol Sci. 2020;21(9):3289.
51. Zarcone MC, Duistermaat E, van Schadewijk A, Jedynska A, Hiemstra PS, Kooter IM. Cellular response of mucociliary differentiated primary bronchial epithelial cells to diesel exhaust. Am J Physiol Lung Cell Mol Physiol. 2016;311(1):L111-23.
52. Xu L, Li X, Wang H, Xie F, Liu H, Xie J. Cigarette smoke triggers inflammation mediated by autophagy in BEAS-2B cells. Ecotoxicol Environ Saf. 2019;184:109617.
53. Chen ZH, Lam HC, Jin Y, Kim HP, Cao J, Lee SJ, et al. Autophagy protein microtubule-associated protein 1 light chain-3B (LC3B) activates extrinsic apoptosis during cigarette smoke-induced

emphysema. Proc Natl Acad Sci U S A. 2010;107(44):18880-5.
54. Ornatowski W, Lu Q, Yegambaram M, Garcia AE, Zemskov EA, Maltepe E, et al. Complex interplay between autophagy and oxidative stress in the development of pulmonary disease. Redox Biol. 2020;36:101679.
55. Yun HR, Jo YH, Kim J, Shin Y, Kim SS, Choi TG. Roles of Autophagy in Oxidative Stress. Int J Mol Sci. 2020;21(9).
56. Malvin NP, Kern JT, Liu T-C, Brody SL, Stappenbeck TS. Autophagy proteins are required for club cell structure and function in airways. American Journal of Physiology-Lung Cellular and Molecular Physiology. 2019;317(2):L259-L70.
57. Li K, Li M, Li W, Yu H, Sun X, Zhang Q, et al. Airway epithelial regeneration requires autophagy and glucose metabolism. Cell Death Dis. 2019;10(12):875.
58. Zhou JS, Zhao Y, Zhou HB, Wang Y, Wu YF, Li ZY, et al. Autophagy plays an essential role in cigarette smoke-induced expression of MUC5AC in airway epithelium. Am J Physiol Lung Cell Mol Physiol. 2016;310(11):L1042-52.
59. Wen W, Yu G, Liu W, Gu L, Chu J, Zhou X, et al. Silencing FUNDC1 alleviates chronic obstructive pulmonary disease by inhibiting mitochondrial autophagy and bronchial epithelium cell apoptosis under hypoxic environment. J Cell Biochem. 2019;120(10):17602-15.
60. Fujita Y, Araya J, Ito S, Kobayashi K, Kosaka N, Yoshioka Y, et al. Suppression of autophagy by extracellular vesicles promotes myofibroblast differentiation in COPD pathogenesis. J Extracell Vesicles. 2015;4:28388.
61. Pampliega O, Cuervo AM. Autophagy and primary cilia: dual interplay. Curr Opin Cell Biol. 2016;39:1-7.
62. Ballweg K, Mutze K, Königshoff M, Eickelberg O, Meiners S. Cigarette smoke extract affects mitochondrial function in alveolar epithelial cells. Am J Physiol Lung Cell Mol Physiol. 2014;307(11):L895-907.
63. Daijo H, Hoshino Y, Kai S, Suzuki K, Nishi K, Matsuo Y, et al. Cigarette smoke reversibly activates hypoxia-inducible factor 1 in a reactive oxygen species-dependent manner. Scientific reports. 2016;6:34424-.
64. Zhang Q, Tang X, Zhang Z-F, Velikina R, Shi S, Le AD. Nicotine induces hypoxia-inducible factor-1α expression in human lung cancer cells via nicotinic acetylcholine receptor–mediated signaling pathways. Clinical Cancer Research. 2007;13(16):4686-94.
65. Yasuo M, Mizuno S, Kraskauskas D, Bogaard HJ, Natarajan R, Cool CD, et al. Hypoxia inducible factor-1α in human emphysema lung tissue. European Respiratory Journal. 2011;37(4):775-83.
66. Ishihara M, Urushido M, Hamada K, Matsumoto T, Shimamura Y, Ogata K, et al. Sestrin-2 and BNIP3 regulate autophagy and mitophagy in renal tubular cells in acute kidney injury. Am J Physiol Renal Physiol. 2013;305(4):F495-509.
67. Bellot G, Garcia-Medina R, Gounon P, Chiche J, Roux D, Pouysségur J, et al. Hypoxia-induced autophagy is mediated through hypoxia-inducible factor induction of BNIP3 and BNIP3L via their BH3 domains. Mol Cell Biol. 2009;29(10):2570-81.
68. Wu W, Li W, Chen H, Jiang L, Zhu R, Feng D. FUNDC1 is a novel mitochondrial-associated-membrane (MAM) protein required for hypoxia-induced mitochondrial fission and mitophagy. Autophagy. 2016;12(9):1675-6.
69. Wang L, Wang P, Dong H, Wang S, Chu H, Yan W, et al. Ulk1/FUNDC1 Prevents Nerve Cells from Hypoxia-Induced Apoptosis by Promoting Cell Autophagy. Neurochemical Research. 2018;43(8):1539-48.

70. Lv M, Wang C, Li F, Peng J, Wen B, Gong Q, et al. Structural insights into the recognition of phosphorylated FUNDC1 by LC3B in mitophagy. Protein Cell. 2017;8(1):25-38.
71. Lee S-J, Kim H-P, Jin Y, Choi AMK, Ryter SW. Beclin 1 deficiency is associated with increased hypoxia-induced angiogenesis. Autophagy. 2011;7(8):829-39.
72. Allen GF, Toth R, James J, Ganley IG. Loss of iron triggers PINK1/Parkin-independent mitophagy. EMBO reports. 2013;14(12):1127-35.
73. Wang X, Yang H, Yanagisawa D, Bellier J-P, Morino K, Zhao S, et al. Mitochondrial ferritin affects mitochondria by stabilizing HIF-1α in retinal pigment epithelium: implications for the pathophysiology of age-related macular degeneration. Neurobiology of aging. 2016;47:168-79.
74. Araya J, Tsubouchi K, Sato N, Ito S, Minagawa S, Hara H, et al. PRKN-regulated mitophagy and cellular senescence during COPD pathogenesis. Autophagy. 2019;15(3):510-26.
75. López-Armada MJ, Riveiro-Naveira RR, Vaamonde-García C, Valcárcel-Ares MN. Mitochondrial dysfunction and the inflammatory response. Mitochondrion. 2013;13(2):106-18.
76. Kampf C, Relova AJ, Sandler S, Roomans GM. Effects of TNF-alpha, IFN-gamma and IL-beta on normal human bronchial epithelial cells. Eur Respir J. 1999;14(1):84-91.
77. Liu Y, Li L, Pan N, Gu J, Qiu Z, Cao G, et al. TNF-α released from retinal Müller cells aggravates retinal pigment epithelium cell apoptosis by upregulating mitophagy during diabetic retinopathy. Biochem Biophys Res Commun. 2021;561:143-50.
78. Vanella L, Li Volti G, Distefano A, Raffaele M, Zingales V, Avola R, et al. A new antioxidant formulation reduces the apoptotic and damaging effect of cigarette smoke extract on human bronchial epithelial cells. Eur Rev Med Pharmacol Sci. 2017;21(23):5478-84.
79. Li J, Dai A, Hu R, Zhu L, Tan S. Positive correlation between PPARgamma/PGC-1alpha and gamma-GCS in lungs of rats and patients with chronic obstructive pulmonary disease. Acta Biochim Biophys Sin. 2010;42(9):603-14.
80. Aravamudan B, Kiel A, Freeman M, Delmotte P, Thompson M, Vassallo R, et al. Cigarette smoke-induced mitochondrial fragmentation and dysfunction in human airway smooth muscle. Am J Physiol Lung Cell Mol Physiol. 2014;306(9):L840-54.
81. Yang D, Xu D, Wang T, Yuan Z, Liu L, Shen Y, et al. Mitoquinone ameliorates cigarette smoke-induced airway inflammation and mucus hypersecretion in mice. Int Immunopharmacol. 2021;90:107149.
82. Solanki HS, Babu N, Jain AP, Bhat MY, Puttamallesh VN, Advani J, et al. Cigarette smoke induces mitochondrial metabolic reprogramming in lung cells. Mitochondrion. 2018;40:58-70.
83. Agarwal AR, Zhao L, Sancheti H, Sundar IK, Rahman I, Cadenas E. Short-term cigarette smoke exposure induces reversible changes in energy metabolism and cellular redox status independent of inflammatory responses in mouse lungs. Am J Physiol Lung Cell Mol Physiol. 2012;303(10):L889-98.
84. Tu C, Mammen MJ, Li J, Shen X, Jiang X, Hu Q, et al. Large-scale, ion-current-based proteomics investigation of bronchoalveolar lavage fluid in chronic obstructive pulmonary disease patients. J Proteome Res. 2014;13(2):627-39.
85. Kao CC, Hsu JW, Bandi V, Hanania NA, Kheradmand F, Jahoor F. Glucose and pyruvate metabolism in severe chronic obstructive pulmonary disease. J Appl Physiol. 2012;112(1):42-7.
86. Pastor MD, Nogal A, Molina-Pinelo S, Meléndez R, Salinas A, González De la Peña M, et al. Identification of proteomic signatures associated with lung cancer and COPD. J Proteomics.

2013;89:227-37.
87. Agarwal AR, Kadam S, Brahme A, Agrawal M, Apte K, Narke G, et al. Systemic Immuno-metabolic alterations in chronic obstructive pulmonary disease (COPD). Respir Res. 2019;20(1):171.
88. Li L, Yang DC, Chen C-H. Metabolic reprogramming: A driver of cigarette smoke-induced inflammatory lung diseases. Free Radical Biology and Medicine. 2021;163:392-401.
89. Zhang W, Wang G, Xu ZG, Tu H, Hu F, Dai J, et al. Lactate Is a Natural Suppressor of RLR Signaling by Targeting MAVS. Cell. 2019;178(1):176-89.e15.
90. Jiang C, Chen Q, Xie M. Smoking increases the risk of infectious diseases: A narrative review. Tob Induc Dis. 2020;18:60.
91. Duffney PF, McCarthy CE, Nogales A, Thatcher TH, Martinez-Sobrido L, Phipps RP, et al. Cigarette smoke dampens antiviral signaling in small airway epithelial cells by disrupting TLR3 cleavage. Am J Physiol Lung Cell Mol Physiol. 2018;314(3):L505-l13.
92. Eddleston J, Lee RU, Doerner AM, Herschbach J, Zuraw BL. Cigarette smoke decreases innate responses of epithelial cells to rhinovirus infection. Am J Respir Cell Mol Biol. 2011;44(1):118-26.
93. Wang Y, Romeo PP, Nikkels J, Ninaber DK, Schrumpf JA, Van Der Does AM, et al. Effect of short-time smoking cessation on rhinovirus-induced innate immune responses in an airway epithelial culture model. ERJ Open Research. 2019;5(suppl 2):PP118.
94. Amatngalim GD, Broekman W, Daniel NM, van der Vlugt LE, van Schadewijk A, Taube C, et al. Cigarette smoke modulates repair and innate immunity following injury to airway epithelial cells. PloS one. 2016;11(11):e0166255.
95. Amatngalim GD, Schrumpf JA, Henic A, Dronkers E, Verhoosel RM, Ordonez SR, et al. Antibacterial defense of human airway epithelial cells from chronic obstructive pulmonary disease patients induced by acute exposure to nontypeable Haemophilus influenzae: modulation by cigarette smoke. Journal of innate immunity. 2017;9(4):359-74.
96. Luppi F, Aarbiou J, van Wetering S, Rahman I, de Boer WI, Rabe KF, et al. Effects of cigarette smoke condensate on proliferation and wound closure of bronchial epithelial cells in vitro: role of glutathione. Respir Res. 2005;6(1):140.
97. Heijink IH, Brandenburg SM, Postma DS, van Oosterhout AJ. Cigarette smoke impairs airway epithelial barrier function and cell–cell contact recovery. European Respiratory Journal. 2012;39(2):419-28.
98. Tatsuta M, Kan-o K, Ishii Y, Yamamoto N, Ogawa T, Fukuyama S, et al. Effects of cigarette smoke on barrier function and tight junction proteins in the bronchial epithelium: protective role of cathelicidin LL-37. Respiratory Research. 2019;20(1):251.
99. Cao X, Wang Y, Xiong R, Muskhelishvili L, Davis K, Richter PA, et al. Cigarette whole smoke solutions disturb mucin homeostasis in a human in vitro airway tissue model. Toxicology. 2018;409:119-28.
100. Gindele JA, Kiechle T, Benediktus K, Birk G, Brendel M, Heinemann F, et al. Intermittent exposure to whole cigarette smoke alters the differentiation of primary small airway epithelial cells in the air-liquid interface culture. Sci Rep. 2020;10(1):6257.
101. Aghapour M, Raee P, Moghaddam SJ, Hiemstra PS, Heijink IH. Airway Epithelial Barrier Dysfunction in Chronic Obstructive Pulmonary Disease: Role of Cigarette Smoke Exposure. Am J Respir Cell Mol Biol. 2018;58(2):157-69.
102. Li L, Yang DC, Chen CH. Metabolic reprogramming: A driver of cigarette smoke-induced inflammatory lung diseases. Free Radic Biol Med. 2021;163:392-401.

103. van der Does AM, Heijink M, Mayboroda OA, Persson LJ, Aanerud M, Bakke P, et al. Dynamic differences in dietary polyunsaturated fatty acid metabolism in sputum of COPD patients and controls. Biochim Biophys Acta Mol Cell Biol Lipids. 2019;1864(3):224-33.
104. Xiong R, Wu Y, Wu Q, Muskhelishvili L, Davis K, Tripathi P, et al. Integration of transcriptome analysis with pathophysiological endpoints to evaluate cigarette smoke toxicity in an in vitro human airway tissue model. Arch Toxicol. 2021;95(5):1739-61.
105. Ishikawa S, Matsumura K, Kitamura N, Takanami Y, Ito S. Multi-omics analysis: Repeated exposure of a 3D bronchial tissue culture to whole-cigarette smoke. Toxicol In Vitro. 2019;54:251-62.

Supplemental figures

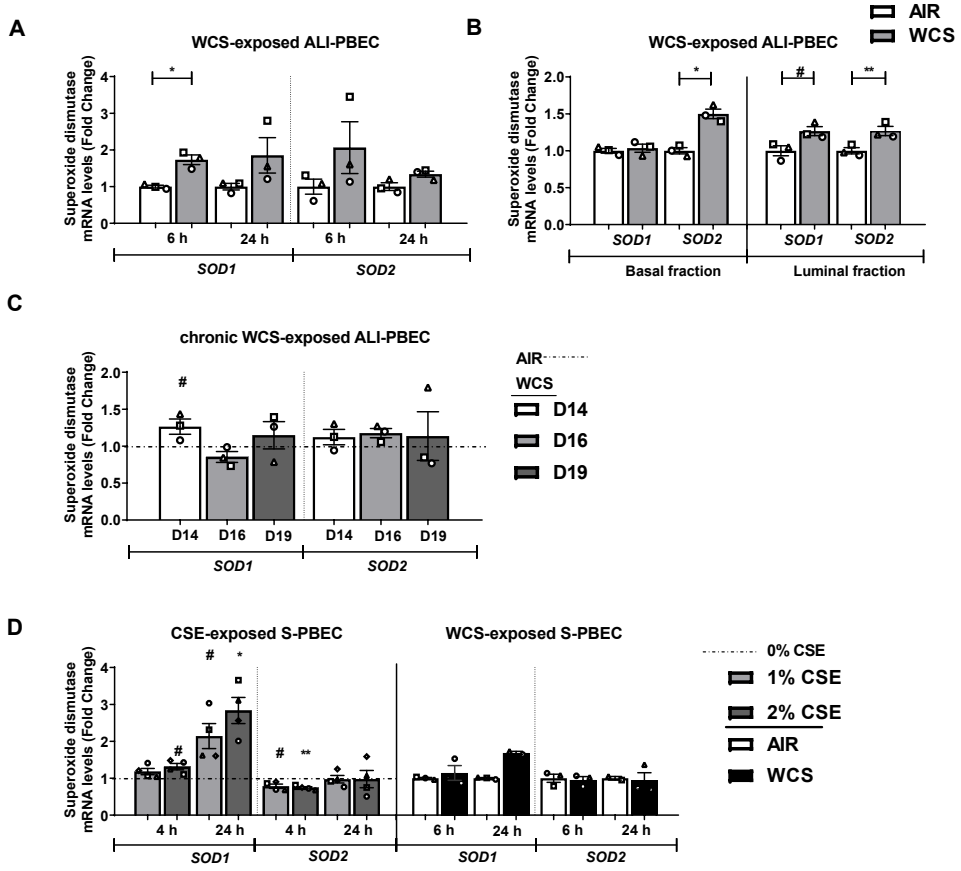

Figure S1. Increase in expression of genes involved in anti-oxidant response after CS exposure in both ALI-and S-PBEC. After 2-weeks of differentiation, ALI-PBEC were exposed to fresh air or WCS from one 3R4F cigarette (University of Kentucky, 2 mg) and whole-cell lysates were harvested after 6 h and 24 h, and the basal and luminal fractions were harvested only at 6 h post-exposure (n=3 donors/group). Gene expression of *SOD1* and *SOD2* in whole-cell lysates of ALI-PBEC (**A**) and separated fractions (**B**) were analyzed by real-time qPCR. ALI-PBEC were 1x daily exposed to fresh air or WCS from one 3R4F cigarette (University of Kentucky, 2 mg) during differentiation for 14 days followed by a cessation period up to 10 days. Cells were harvested on Day 14 (24 hours after the last WCS exposure), 16 and 19 (n=3 donors/group). mRNA levels of *SOD1* and *SOD2* **(C)** were analyzed in whole-cell lysates. Undifferentiated S-PBEC were treated with CSE from one 3R4F cigarette (University of Kentucky) diluted in HBSS (0-1-2%) in Lonza starvation medium for 4 h or 24 h (n=4 donors/group) or undifferentiated S-PBEC cultured on transwells were exposed, after removal of apical medium, to fresh air or WCS from one 3R4F cigarette (University of Kentucky, 2 mg) followed by harvesting of whole-cell lysates after 6 h or 24 h recovery (n=2-3 donors/group). mRNA levels of *SOD1* and *SOD2* **(D)** were analyzed in whole-cell lysates. Data are presented as mean fold change compared to control

(air, 0% CSE or WCS Day 14) ± s.e.m.. Independent donors are represented by open circles, triangles, squares or diamonds. In case of the CSE-exposed S-PBEC experiments, the symbols reflect the mean of technical triplicates. Statistical differences between WCS versus air or WCS versus air after smoking cessation in ALI-PBEC on each day (e.g., WCS Day 14 versus air). were tested using a two-tailed paired parametric *t*-test. If comparison of various groups was required in case of the CSE exposure (CSE 1% or 2% versus 0% CSE) or in WCS chronic smoking cessation experiments (WCS Day 16, 19 versus WCS Day 14), an one-way ANOVA (matched/repeated measures) followed by Sidak's post-hoc test for multiple comparisons was conducted, and in case of missing values the mixed-effects models was performed. Statistical significance is indicated as $^{\#}p<0.1$, $^{*}p<0.05$ and $^{**}p<0.01$ compared to control (air, 0% CSE or WCS Day 14).

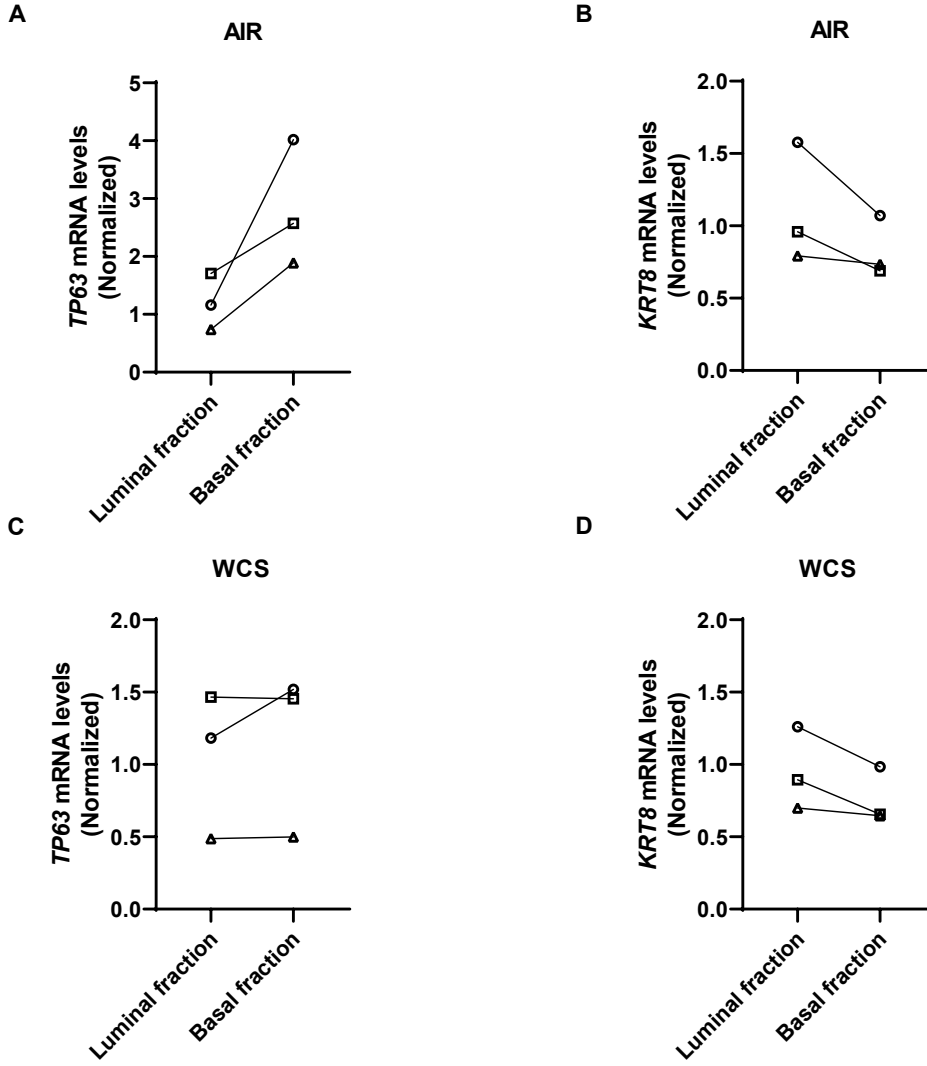

Figure S2. Validation of separation of basal and luminal cell fractions from ALI-PBEC. After 2-weeks of differentiation, ALI-PBEC were exposed to fresh air or WCS from one 3R4F cigarette (University of Kentucky, 2 mg) and separated into luminal and basal cell fractions at 6 h post-exposure using calcium depletion followed by trypsinization (n=3 donors/group). Independent donors are represented by open circles, triangles or squares. Successful separation was identified by measuring gene expression of basal cells marker (Tp63) **(A, C)** and early progenitor cell marker (cytokeratin-8, KRT8) **(B, D)**.

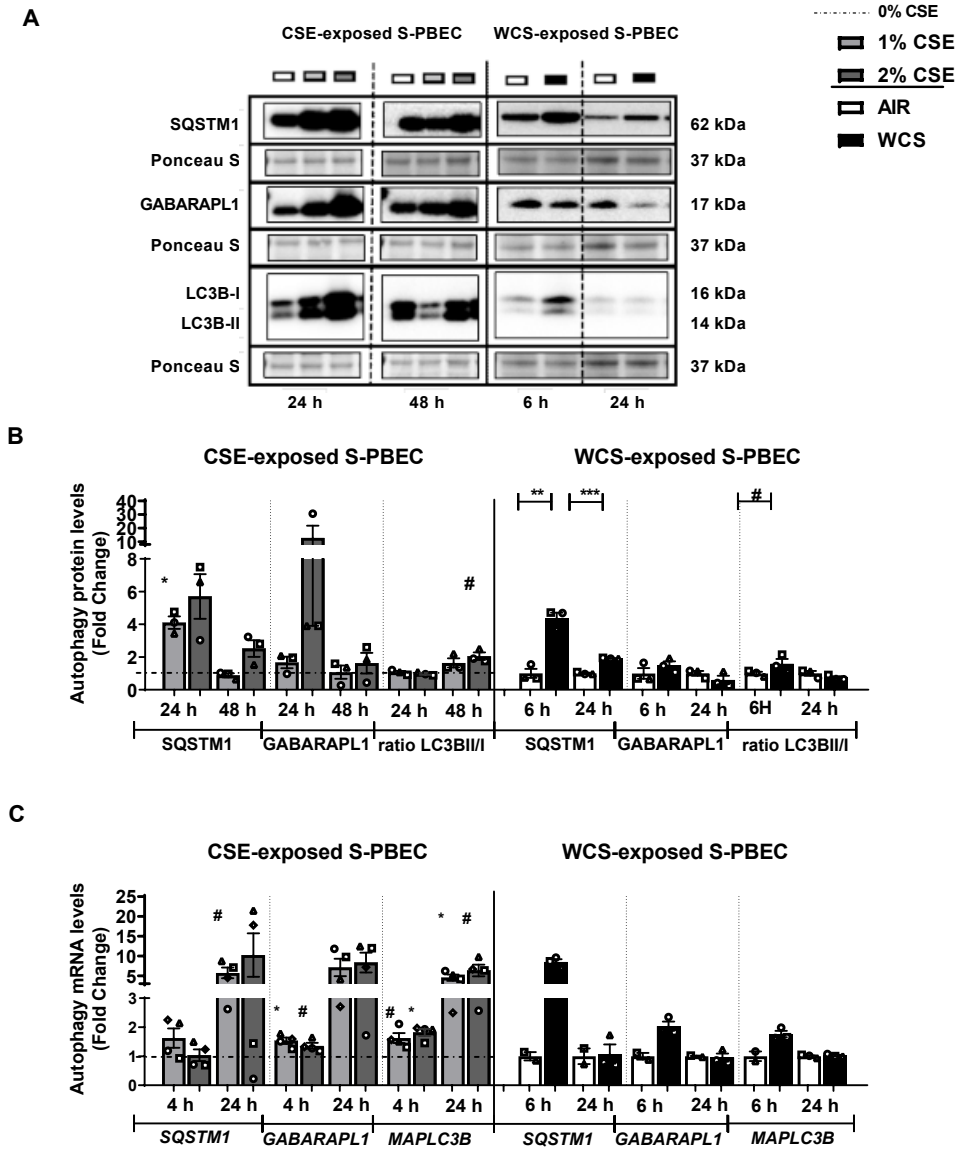

Figure S3. Increase in abundance of key constituents involved in autophagy following acute CSE or WCS exposure in S-PBEC. Undifferentiated S-PBEC were treated with CSE from one 3R4F cigarette (University of Kentucky) diluted in HBSS (0-1-2%) in Lonza starvation medium for 4 h, 24 h or 48 h (n=3-4 donors/group) or undifferentiated S-PBEC cultured on transwells were exposed, after removal of apical medium, to fresh air or WCS from one 3R4F cigarette (University of Kentucky, 2 mg) followed by harvesting of whole-cell lysates after 6 h or 24 h recovery (n=2-3 donors/group). Protein **(A, B)** as well as transcript abundance **(C)** of autophagy regulators SQSTM1, GABARAPL1 and ratio LC3BII/I or MAP1LC3B were measured by western blot and real-time qPCR. Representative western blots, including representative parts of the Ponceau S Staining, are shown. Data are presented as mean fold change compared to control (0% CSE or air) ± s.e.m.. Independent donors are represented by open circles, triangles, squares or diamonds. In case of the CSE-exposed S-PBEC experiments, the symbols reflect the mean of technical triplicates. Statistical differences between the various CSE exposure groups (CSE 1% or 2% versus 0% CSE) were tested using an one-way ANOVA (matched/ repeated measures) followed by Sidak's post-hoc test for multiple comparisons, and in case of missing values the mixed-effects models was performed. WCS versus air was tested using a two-tailed paired parametric *t*-test. Statistical significance is indicated as $^{\#}p<0.1$, $^{*}p<0.05$ and $^{**}p<0.01$ compared to control (0% CSE or air).

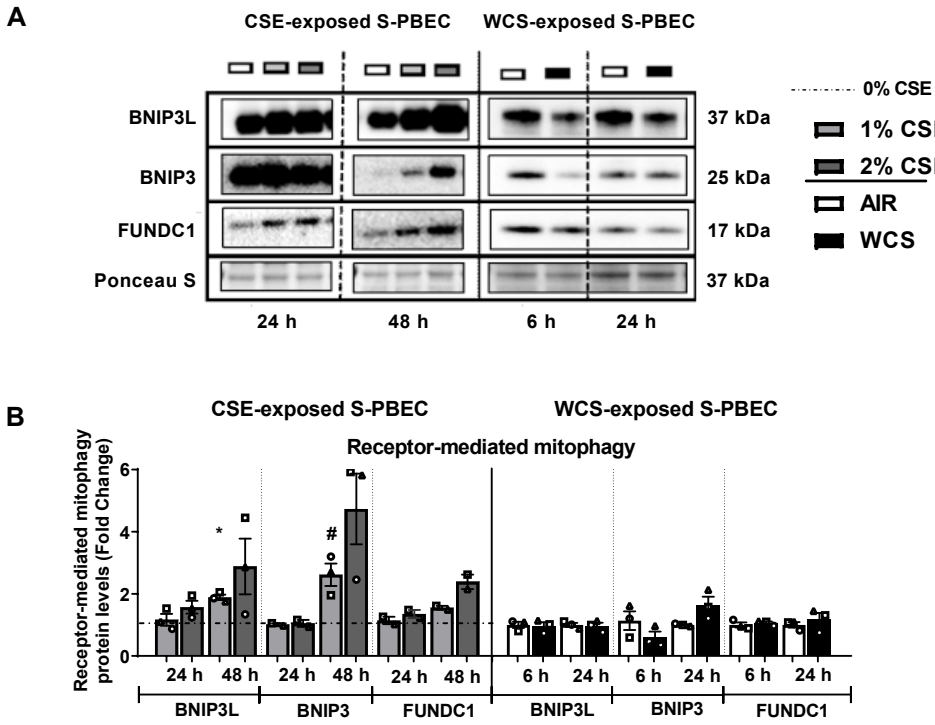

Continued to next page

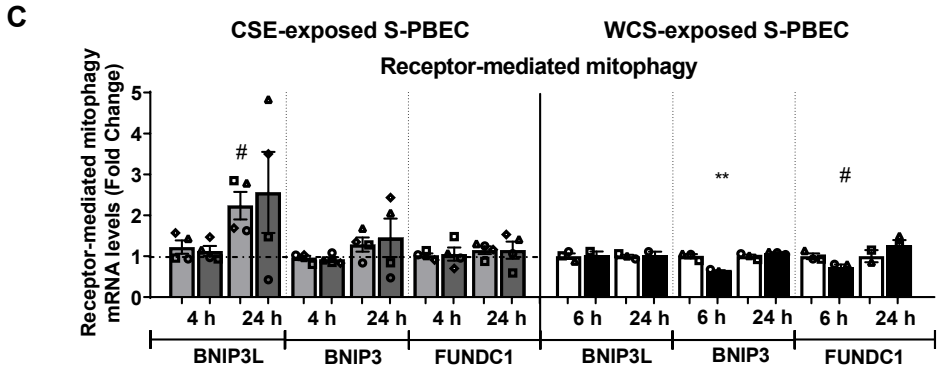

Figure S4. Upregulation of constituents of the receptor-mediated mitophagy machinery in CS-exposed S-PBEC. Undifferentiated S-PBEC were treated with CSE from one 3R4F cigarette (University of Kentucky) diluted in HBSS (0-1-2%) in Lonza starvation medium for 4 h, 24 h or 48 h (n=2-4 donors/group) or undifferentiated S-PBEC cultured on transwells were exposed, after removal of apical medium, to fresh air or WCS from one 3R4F cigarette (University of Kentucky, 2 mg) followed by harvesting of whole-cell lysates after 6 h or 24 h recovery (n=2-3 donors/group). Protein **(A, B)** and mRNA levels **(C)** of regulators involved in receptor-mediated mitophagy (BNIP3L, BNIP3, FUNDC1) were analyzed in whole-cell lysates. Representative western blots, including representative parts of the Ponceau S Staining, are shown. Data are presented as mean fold change compared to control (0% CSE or air) ± s.e.m.. Independent donors are represented by open circles, triangles, squares or diamonds. In case of the CSE-exposed S-PBEC experiments, the symbols reflect the mean of technical triplicates. Statistical differences between the various CSE exposure groups (CSE 1% or 2% versus 0% CSE) were tested using an one-way ANOVA (matched/repeated measures) followed by Sidak's post-hoc test for multiple comparisons, and in case of missing values the mixed-effects models was performed. WCS versus air was tested using a two-tailed paired parametric *t*-test. Statistical significance is indicated as $^{\#}p<0.1$, $^{*}p<0.05$ and $^{**}p<0.01$ compared to control (0% CSE or air).

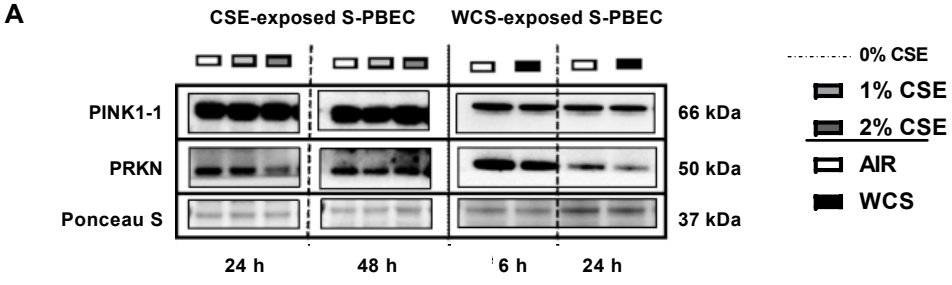

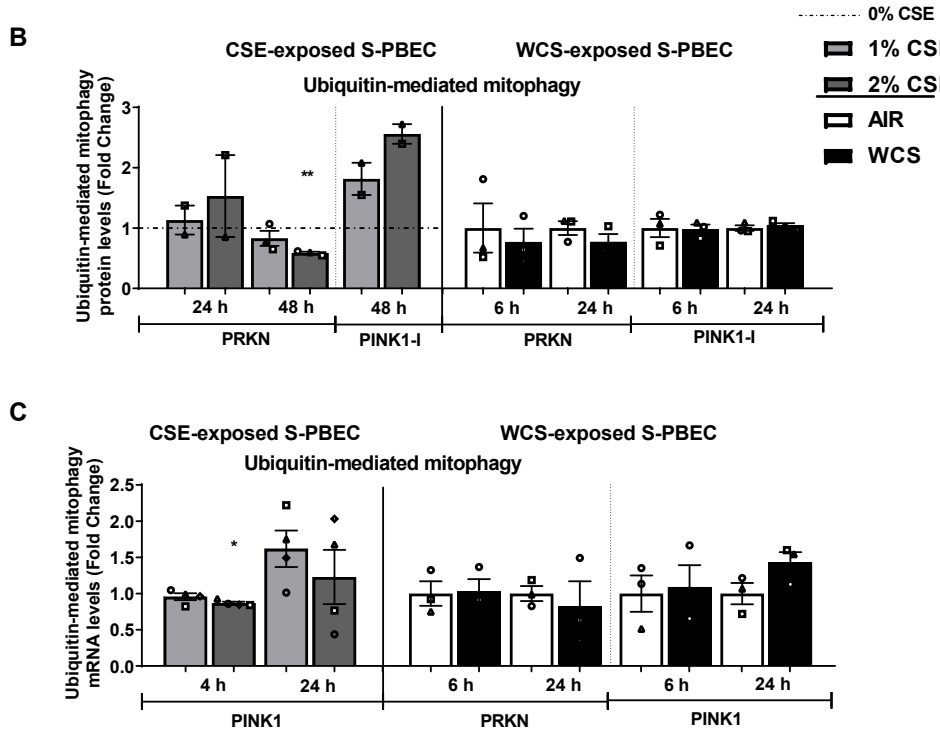

Figure S5. Modulation of ubiquitin-mediated mitophagy markers in CS-exposed S-PBEC. Undifferentiated S-PBEC were treated with CSE from one 3R4F cigarette (University of Kentucky) diluted in HBSS (0-1-2%) in Lonza starvation medium for 4 h, 24 h or 48 h (n=2-4 donors/group) or undifferentiated S-PBEC cultured on transwells were exposed, after removal of apical medium, to fresh air or WCS from one 3R4F cigarette (University of Kentucky, 2 mg) followed by harvesting of whole-cell lysates after 6 h or 24 h recovery (n=3 donors/group). Protein **(A, B)** and mRNA levels **(C)** of regulators involved in ubiquitin-mediated mitophagy (PRKN, PINK1) were analyzed in whole-cell lysates. Western blot analysis revealed one distinct band for PINK1 protein corresponding with expected molecular weight for PINK1-I (66 kDa). Representative western blots, including representative parts of the Ponceau S Staining, are shown. Data are presented as mean fold change compared to control (0% CSE or air) ± s.e.m.. Independent donors are represented by open circles, triangles, squares or diamonds. In case of the CSE-exposed S-PBEC experiments, the symbols reflect the mean of technical triplicates. Statistical differences between the various CSE exposure groups (CSE 1% or 2% versus 0% CSE) were tested using an one-way ANOVA (matched/repeated measures) followed by Sidak's post-hoc test for multiple comparisons, and in case of missing values the mixed-effects models was performed. WCS versus air was tested using a two-tailed paired parametric *t*-test. Statistical significance is indicated as *p<0.05 and **p<0.01 compared to control (0% CSE or air).

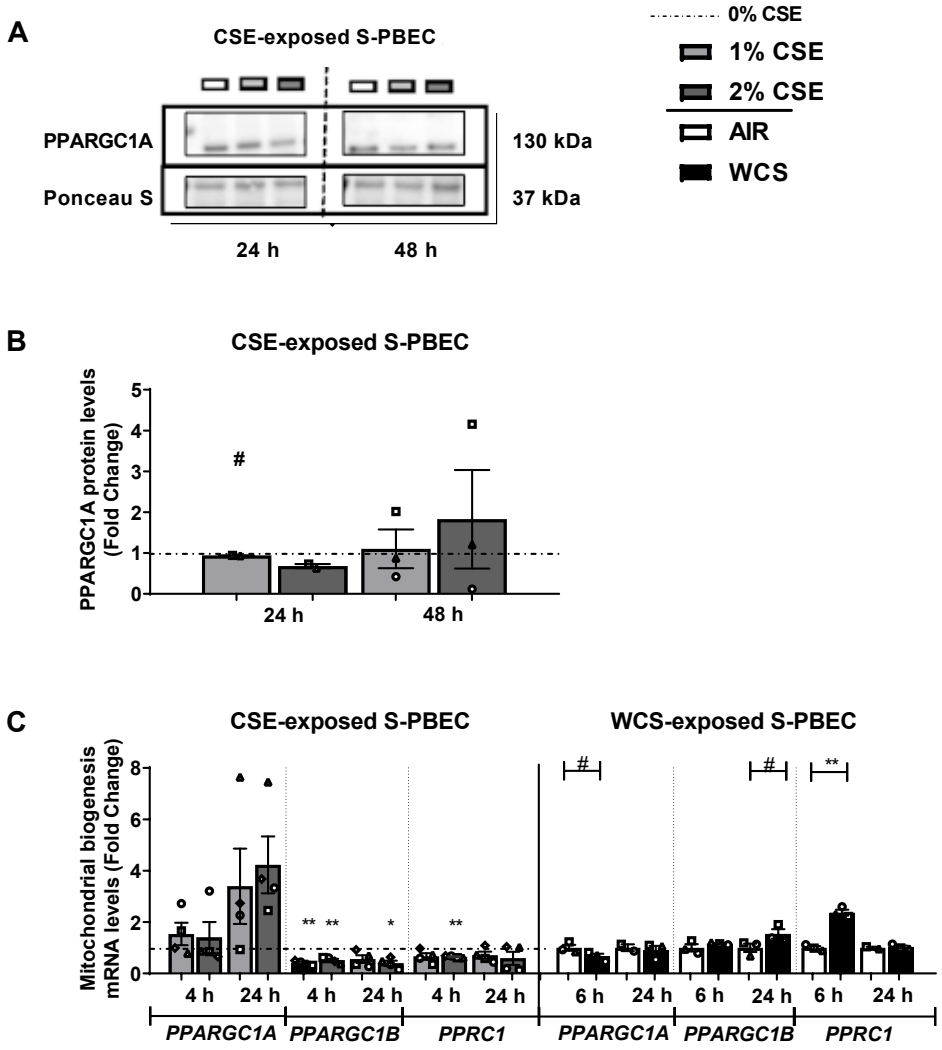

Figure S6. Alterations in expression of transcript levels of transcriptional co-activators of the PPARGC1 network in response to acute CS exposure in S-PBEC. Undifferentiated S-PBEC were treated with CSE from one 3R4F cigarette (University of Kentucky) diluted in HBSS (0-1-2%) in Lonza starvation medium for 4 h, 24 h or 48 h (n=2-4 donors/group) or undifferentiated S-PBEC cultured on transwells were exposed, after removal of apical medium, to fresh air or WCS from one 3R4F cigarette (University of Kentucky, 2 mg) followed by harvesting of whole-cell lysates after 6 h or 24 h recovery (n=2-3 donors/group). Protein **(A, B)** as well as transcript abundance **(C)** of transcriptional co-activators involved in the PPARGC1 network (PPARGC1A, PPARGC1B, PPRC1) are presented. Representative western blots, including representative parts of the Ponceau S Staining, are shown. Data are presented as mean fold change compared to control (0% CSE or air) ± s.e.m.. Independent donors are represented by open circles, triangles, squares or diamonds. In case of the CSE-exposed S-PBEC experiments, the

symbols reflect the mean of technical triplicates. Statistical differences between the various CSE exposure groups (CSE 1% or 2% versus 0% CSE) were tested using an one-way ANOVA (matched/ repeated measures) followed by Sidak's post-hoc test for multiple comparisons, and in case of missing values the mixed-effects models was performed. WCS versus air was tested using a two-tailed paired parametric t-test. Statistical significance is indicated as $^{\#}p<0.1$, $^{*}p<0.05$ and $^{**}p<0.01$ compared to control (0% CSE or air).

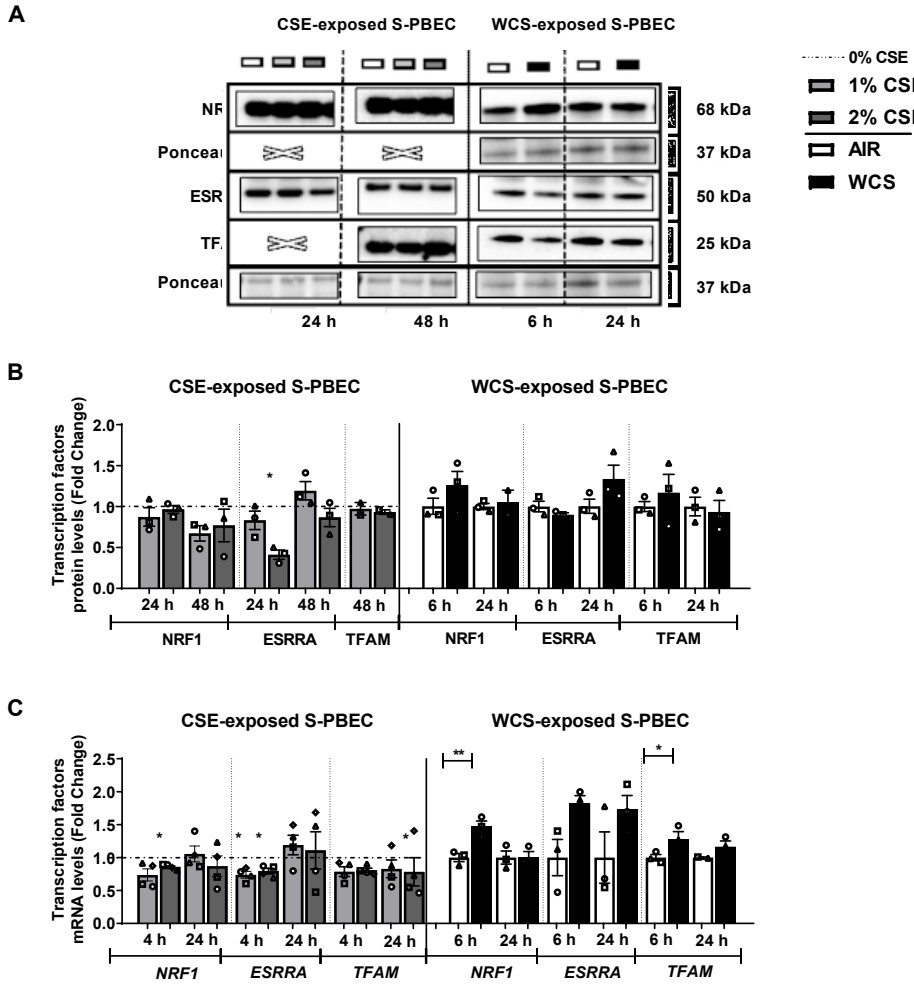

Figure S7. Changes in the abundance of PPARGC1-coactivated transcription factors after CS exposure in S-PBEC. Undifferentiated S-PBEC were treated with CSE from one 3R4F cigarette (University of Kentucky) diluted in HBSS (0-1-2%) in Lonza starvation medium for 4 h, 24 h or 48 h (n=3-4 donors/ group) or undifferentiated S-PBEC cultured on transwells were exposed, after removal of apical medium, to fresh air or WCS from one 3R4F cigarette (University of Kentucky, 2 mg) followed by harvesting of

whole-cell lysates after 6 h or 24 h recovery (n=2-3 donors/group). Protein **(A, B)** and mRNA levels **(C)** of PPARGC1-coactivated transcription regulators, NRF1, ESRRA and TFAM, were measured by western blotting or real-time qPCR. Representative western blots, including representative parts of the Ponceau S Staining, are shown. Data are presented as mean fold change compared to control (0% CSE or air) ± s.e.m.. Independent donors are represented by open circles, triangles, squares or diamonds. In case of the CSE-exposed S-PBEC experiments, the symbols reflect the mean of technical triplicates. Statistical differences between the various CSE exposure groups (CSE 1% or 2% versus 0% CSE) were tested using an one-way ANOVA (matched/repeated measures) followed by Sidak's post-hoc test for multiple comparisons, and in case of missing values the mixed-effects models was performed. WCS versus air was tested using a two-tailed paired parametric *t*-test. Statistical significance is indicated as *p<0.05 and **p<0.01 compared to control (0% CSE or air).

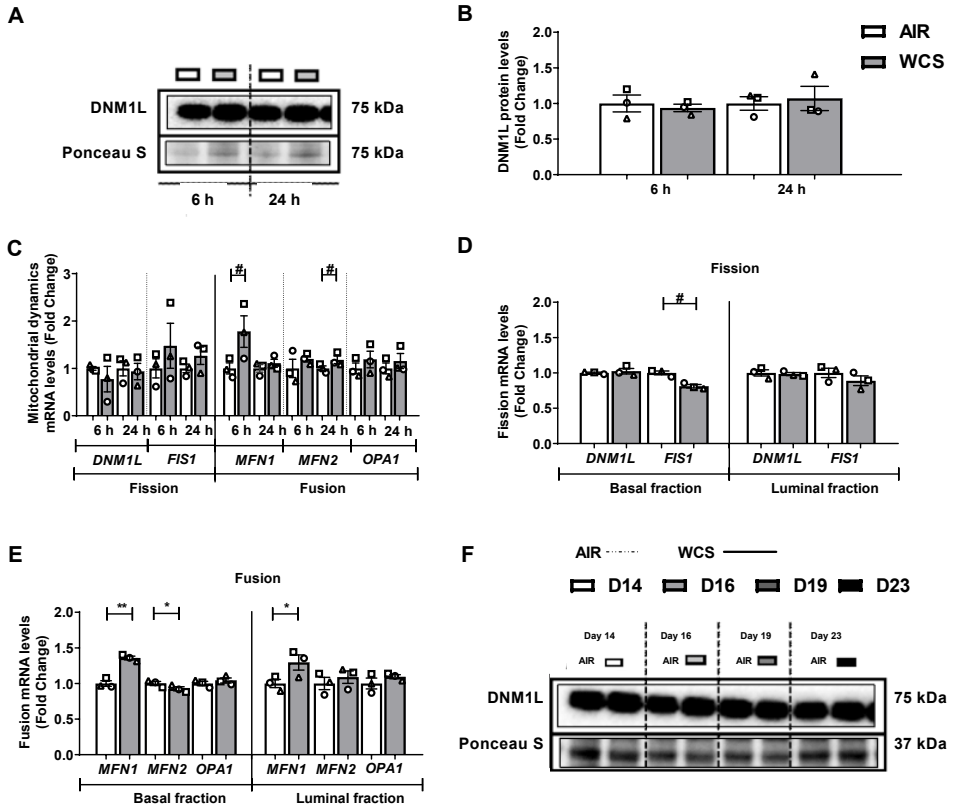

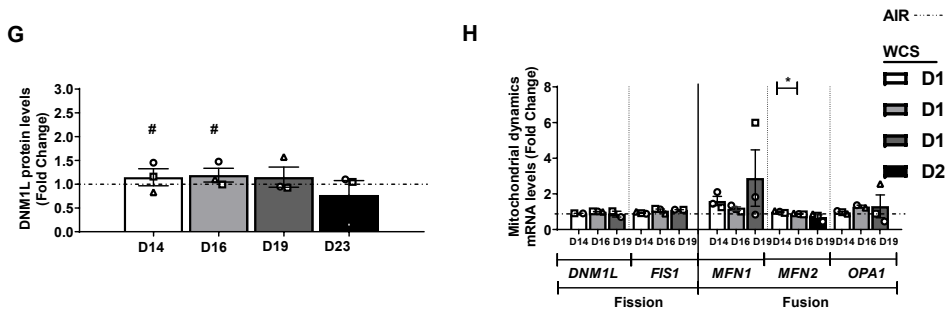

Figure S8. Changes in mitochondrial dynamics markers in response to WCS exposure in ALI-PBEC. After 2-weeks of differentiation, ALI-PBEC were exposed to fresh air or WCS from one 3R4F cigarette (University of Kentucky, 2 mg) and whole-cell lysates were harvested after 6 h and 24 h, and the basal and luminal fractions were harvested only at 6 h post-exposure (n=3 donors/group). Protein **(A, B)** and mRNA levels **(C, D, E)** of fission- and fusion-associated markers were analyzed in whole-cell lysates or basal/luminal cell fractions post-exposure. Data are presented as mean fold change compared to control (air) ± s.e.m.. Independent donors are represented by open circles, triangles or squares. Statistical differences between WCS versus air were tested using a two-tailed paired parametric *t*-test, $^{\#}p<0.1$, $^{*}p<0.05$ and $^{**}p<0.01$. ALI-PBEC were 1x daily exposed to fresh air or WCS from one 3R4F cigarette (University of Kentucky, 2 mg) during differentiation for 14 days followed by a cessation period up to 10 days. Cells were harvested on Day 14 (24 h after the last exposure), 16, 19 and 23 (n=2-3 donors/group). Abundance of DNM1L protein **(F, G)** and transcript abundance of fission and fusion regulators **(H)** are shown. Representative western blots, including representative parts of the Ponceau S Staining, are shown. Data are presented as mean fold change compared to control (air or WCS Day 14) ± s.e.m.. Independent donors are represented by open circles, triangles or squares. Statistical differences between WCS versus air after smoking cessation in ALI-PBEC on each day was tested using a two-tailed paired parametric *t*-test (e.g., WCS Day 14 versus air). Comparison of various groups to test the difference of WCS Day 16, 19, 23 versus Day 14 in WCS chronic smoking cessation experiments was conducted using an one-way ANOVA followed by Sidak's post-hoc test for multiple comparisons, and in case of missing values the mixed-effects models was performed. Statistical significance is indicated as $^{\#}p<0.1$ and $^{*}p<0.05$ compared to control (air or WCS Day 14).

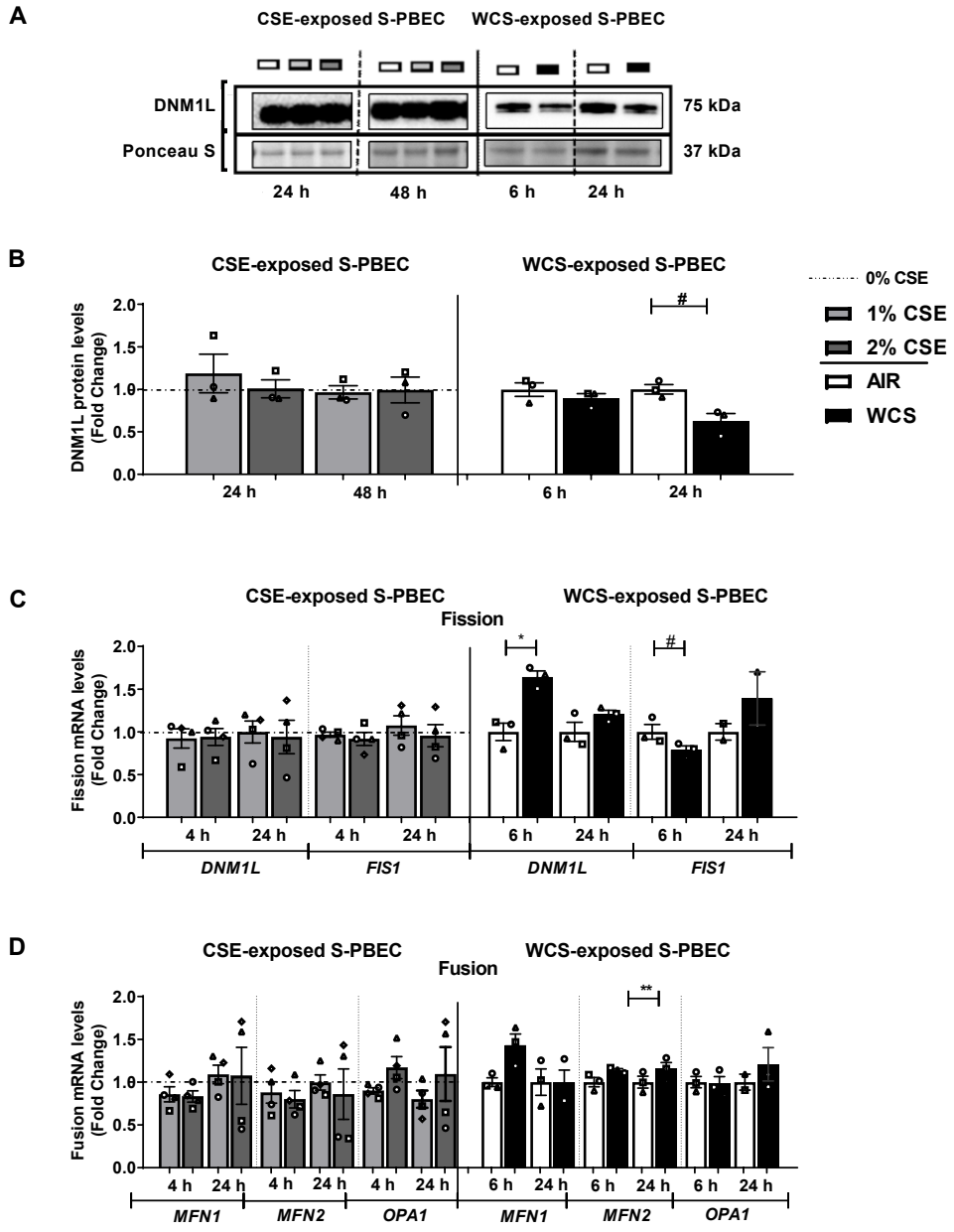

Figure S9. Aberrant protein and transcript abundance of fission- and fusion-associated markers in S-PBEC. Undifferentiated S-PBEC were treated with CSE from one 3R4F cigarette (University of Kentucky) diluted in HBSS (0-1-2%) in Lonza starvation medium for 4 h, 24 h or 48 h (n=3-4 donors/group) or undifferentiated S-PBEC cultured on transwells were exposed, after removal of apical medium, to fresh air or WCS from one 3R4F cigarette (University of Kentucky, 2 mg) followed by harvesting of whole-

cell lysates after 6 h or 24 h recovery (n=2-3 donors/group). Protein **(A, B)** and mRNA levels **(C)** of fission-associated markers (DNM1L, FIS1) and gene expression of fusion-associated markers (MFN1, MFN2, OPA1) **(D)** were measured using western blot and real-time qPCR. Representative western blots, including representative parts of the Ponceau S Staining, are shown. Data are presented as mean fold change compared to control (0% CSE or air) ± s.e.m.. Independent donors are represented by open circles, triangles, squares or diamonds. In case of the CSE-exposed S-PBEC experiments, the symbols reflect the mean of technical triplicates. Statistical differences between the various CSE exposure groups (CSE 1% or 2% versus 0% CSE) were tested using an one-way ANOVA (matched/ repeated measures) followed by Sidak's post-hoc test for multiple comparisons, and in case of missing values the mixed-effects models was performed. WCS versus air was tested using a two-tailed paired parametric *t*-test. Statistical significance is indicated as $^{\#}p<0.1$, *p<0.05 and **p<0.01 compared to control (0% CSE or air).

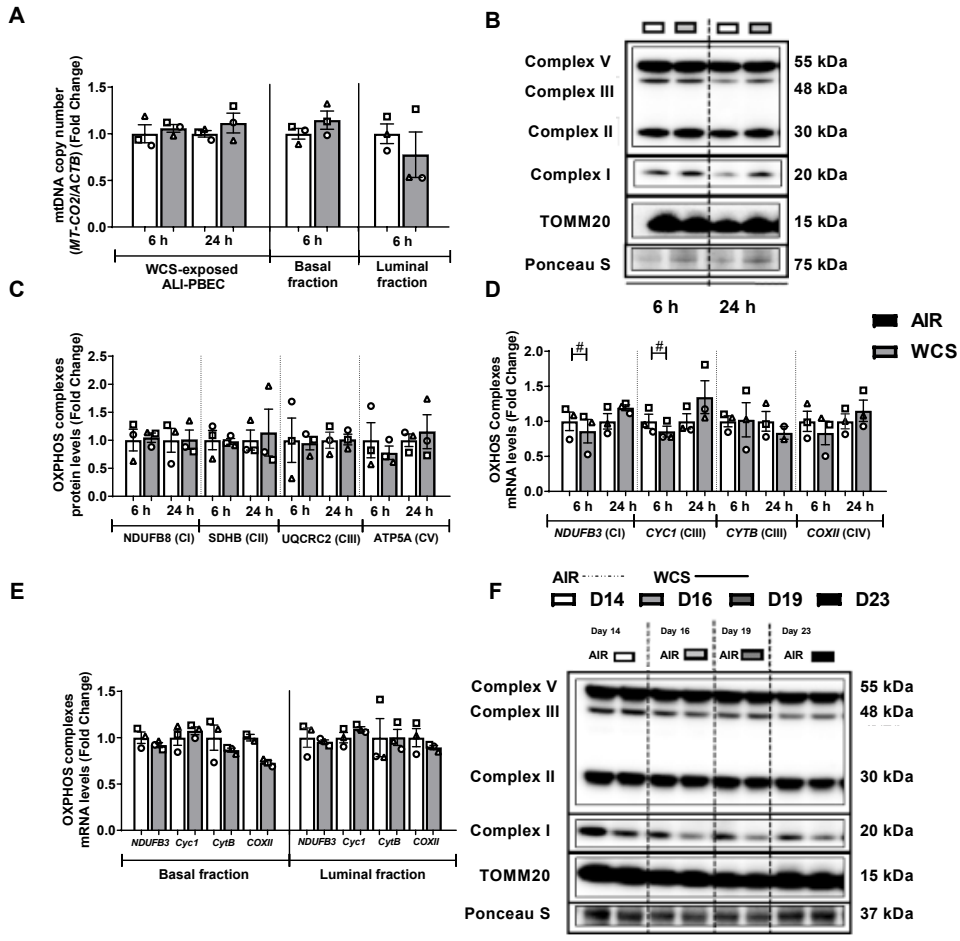

Continued to next page

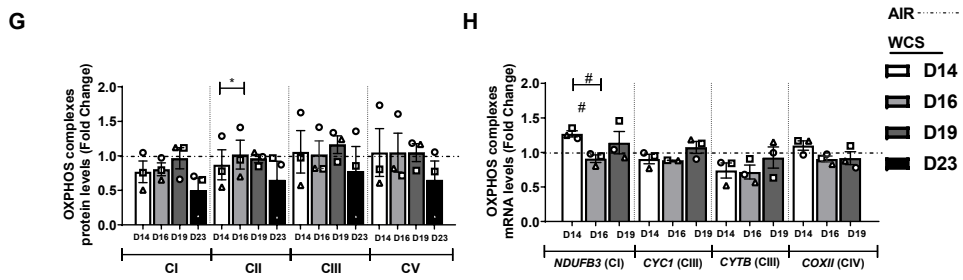

Figure S10. Unaltered abundance of subunits of the electron transport chain in WCS-exposed ALI-PBEC. After 2-weeks of differentiation, ALI-PBEC were exposed to fresh air or WCS from one 3R4F cigarette (University of Kentucky, 2 mg) and whole-cell lysates were harvested after 6 h and 24 h, and the basal and luminal fractions were harvested only at 6 h post-exposure (n=2-3 donors/group). Mitochondrial DNA copy number **(A)**, protein **(B, C)** as well as transcript levels **(D, E)** of nuclear and mitochondrial-encoded subunits of the electron transport chain (Complex I (CI), Complex II (CII), Complex III (CIII), Complex IV (CIV), Complex V (CV)) were analyzed in whole-cell lysates or basal and luminal fractions post-exposure. Data are presented as mean fold change compared to control (air) ± s.e.m.. Independent donors are represented by open circles, triangles or squares. Statistical differences between WCS versus air were tested using a two-tailed paired parametric *t*-test, $^{\#}p<0.1$. ALI-PBEC were 1x daily exposed to fresh air or WCS from one 3R4F cigarette (University of Kentucky, 2 mg) during differentiation for 14 days followed by a cessation period up to 10 days. Cells were harvested on Day 14 (24 h after the last exposure), 16, 19 and 23 (n=2-3 donors/group). Protein **(F, G)** and mRNA expression **(H)** of subunits of the electron transport chain are analyzed. Representative western blots, including representative parts of the Ponceau S Staining, are shown. Data are presented as mean fold change compared to control (air or WCS Day 14) ± s.e.m.. Independent donors are represented by open circles, triangles or squares. Statistical differences between WCS versus air after smoking cessation in ALI-PBEC on each day was tested using a two-tailed paired parametric *t*-test (e.g, WCS Day 14 versus air). Comparison of various groups to test the difference of WCS Day 16, 19, 23 versus Day 14 in WCS chronic smoking cessation experiments was conducted using an one-way ANOVA followed by Sidak's post-hoc test for multiple comparisons, and in case of missing values the mixed-effects models was performed. Statistical significance is indicated as $^{\#}p<0.1$ and $^{*}p<0.05$ compared to control (air or WCS Day 14).

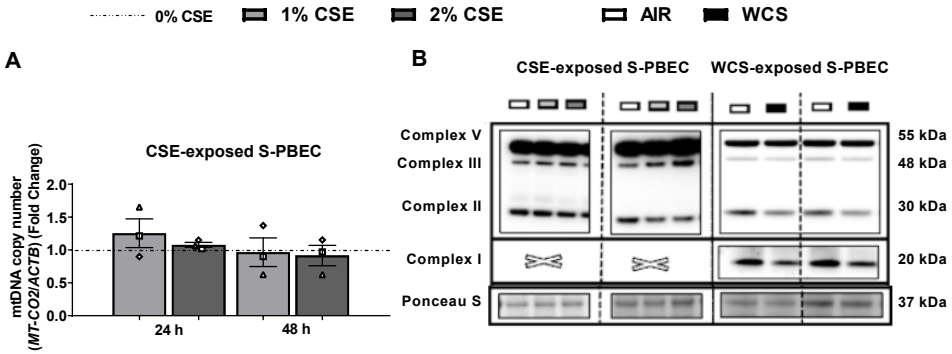

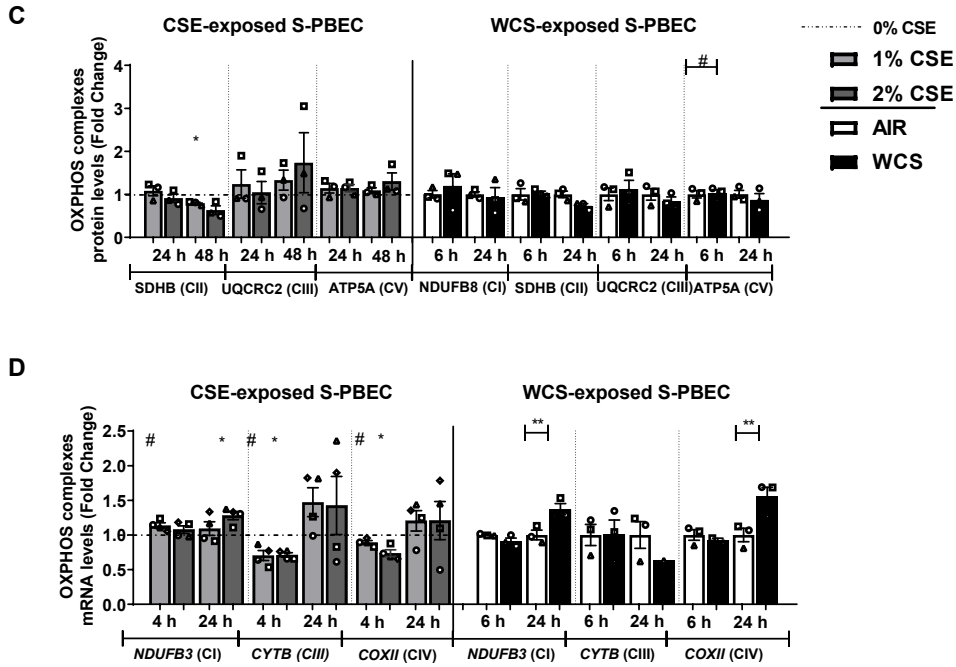

Figure S11. Modulation in the abundance of subunits of the electron transport chain in CS-exposed S-PBEC. Undifferentiated S-PBEC were treated with CSE from one 3R4F cigarette (University of Kentucky) diluted in HBSS (0-1-2%) in Lonza starvation medium for 4 h, 24 h or 48 h (n=3-4 donors/group) or undifferentiated S-PBEC cultured on transwells were exposed, after removal of apical medium, to fresh air or WCS from one 3R4F cigarette (University of Kentucky, 2 mg) followed by harvesting of whole-cell lysates after 6 h or 24 h recovery (n=1-3 donors/group). Mitochondrial DNA copy number **(A)**, protein **(B, C)** as well as transcript levels **(D)** of nuclear and mitochondrial-encoded subunits of the electron transport chain (Complex I (CI), Complex II (CII), Complex III (CIII), Complex IV (CIV), Complex V (CV)) were analyzed in whole-cell lysates. Representative western blots, including representative parts of the Ponceau S Staining, are shown. Data are presented as mean fold change compared to control (0% CSE or air) ± s.e.m.. Independent donors are represented by open circles, triangles, squares or diamonds. In case of the CSE-exposed S-PBEC experiments, the symbols reflect the mean of technical triplicates. Statistical differences between the various CSE exposure groups (CSE 1% or 2% versus 0% CSE) were tested using an one-way ANOVA (matched/repeated measures) followed by Sidak's post-hoc test for multiple comparisons, and in case of missing values the mixed-effects models was performed. WCS versus air was tested using a two-tailed paired parametric *t*-test. Statistical significance is indicated as $^{\#}p<0.1$, $^{*}p<0.05$ and $^{**}p<0.01$ compared to control (0% CSE or air).

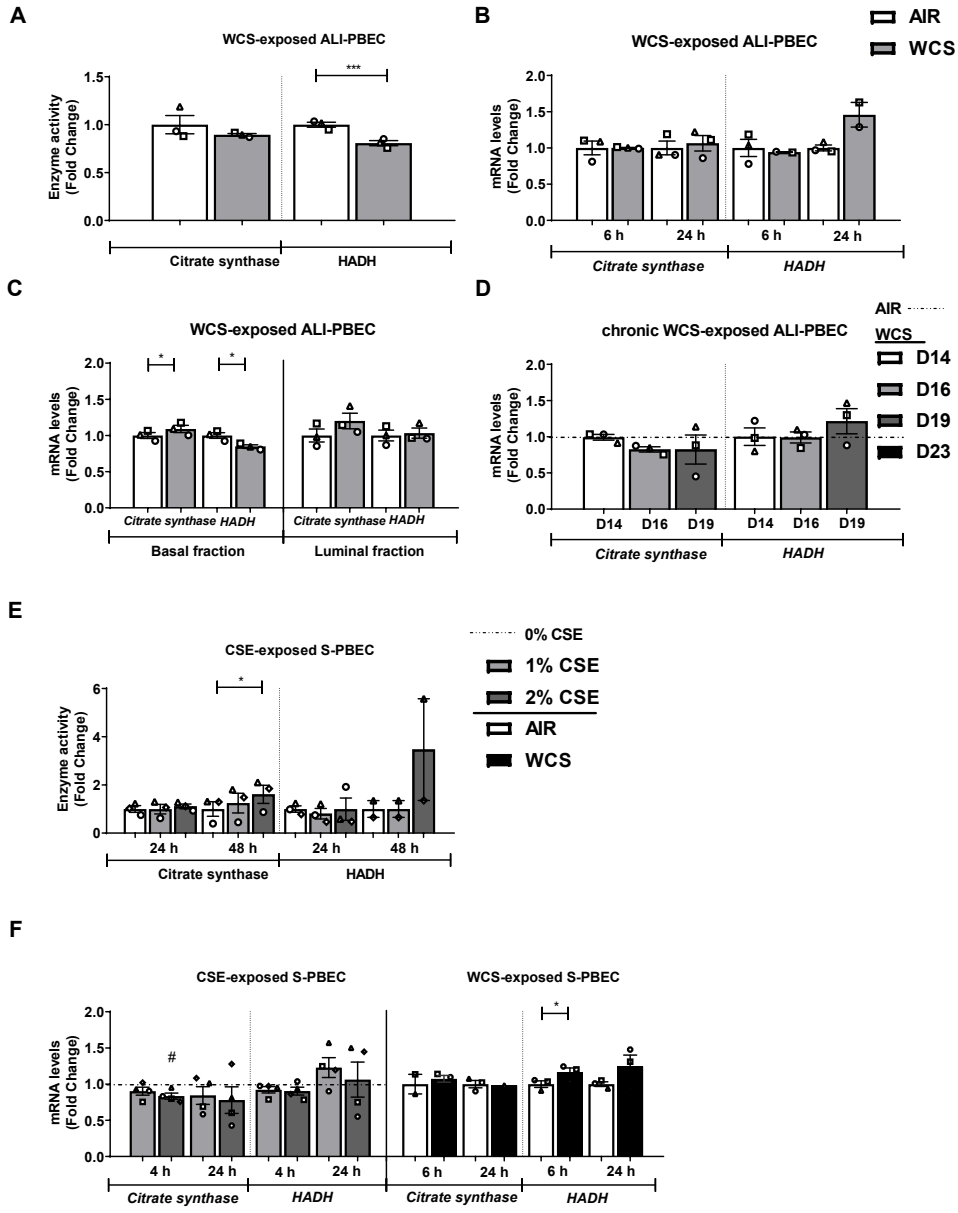

Figure S12. Disruption of activity and abundance of key components involved in the fatty acid β-oxidation in CS-exposed ALI- and S-PBEC. After 2-weeks of differentiation, ALI-PBEC were exposed to fresh air or WCS from one 3R4F cigarette (University of Kentucky, 2 mg) and whole-cell lysates were harvested after 6 h and 24 h, and the basal and luminal fractions were harvested only at 6 h post-exposure (n=2-3 donors/group). Enzyme activities of citrate synthase and HADH **(A)** and related transcript abundance in whole-cell lysates **(B)** or basal and luminal fractions **(C)** were assessed in ALI-PBEC. Next, ALI-PBEC were 1x daily exposed to fresh air or WCS from one 3R4F cigarette (University of

Kentucky, 2 mg) during differentiation for 14 days followed by a cessation period up to 10 days. Cells were harvested on Day 14 (24 h after the last exposure), 16 and 19 (n=3 donors/group). Transcript abundance **(D)** of *citrate synthase* and *HADH* were measured. Undifferentiated S-PBEC were treated with CSE from one 3R4F cigarette (University of Kentucky) diluted in HBSS (0-1-2%) in Lonza starvation medium for 4 h, 24 h or 48 h (n=4 donors/group) or undifferentiated S-PBEC cultured on transwells were exposed, after removal of apical medium, to fresh air or WCS from one 3R4F cigarette (University of Kentucky, 2 mg) followed by harvesting of whole-cell lysates after 6 h or 24 h recovery (n=1-3 donors/group). Cell lysates were used to measure enzyme activities of citrate synthase and HADH **(E)** and related transcript abundance **(F)**. Data are presented as mean fold change compared to control (air, 0% CSE or WCS Day 14) ± s.e.m.. Independent donors are represented by open circles, triangles, squares or diamonds. In case of the CSE-exposed S-PBEC experiments, the symbols reflect the mean of technical triplicates. Statistical differences between WCS versus air or WCS versus air after smoking cessation in ALI-PBEC on each day (e.g., WCS Day 14 versus air) were tested using a two-tailed paired parametric *t*-test. If comparison of various groups was required in case of the CSE exposure (CSE 1% or 2% versus 0% CSE) or in WCS chronic smoking cessation experiments (WCS Day 16, 19 versus WCS Day 14), an one-way ANOVA (matched/repeated measures) followed by Sidak's post-hoc test for multiple comparisons was conducted, and in case of missing values the mixed-effects models was performed. Statistical significance is indicated as $^{\#}p<0.1$, *p<0.05 and **p<0.01 compared to control (air, 0% CSE or WCS Day 14).

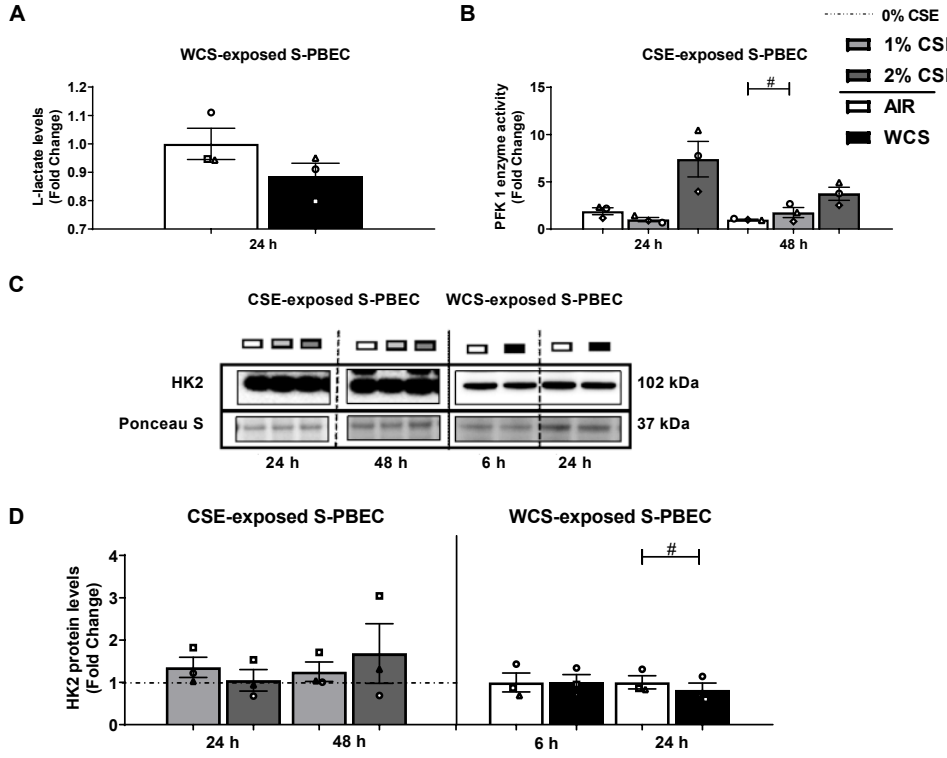

Continued to next page

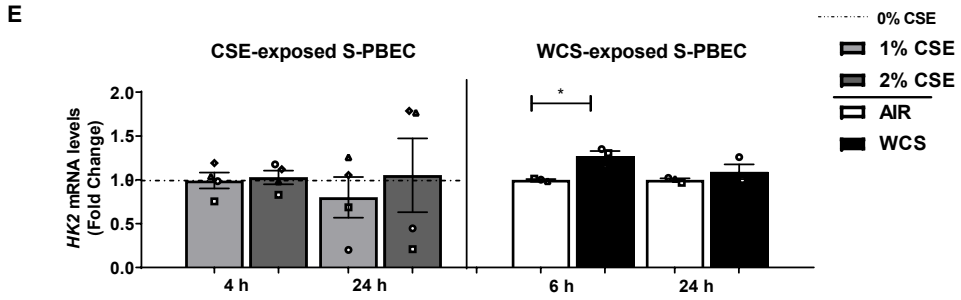

Figure S13. Glycolytic shift after CS exposure in S-PBEC. Undifferentiated S-PBEC were treated with CSE from one 3R4F cigarette (University of Kentucky) diluted in HBSS (0-1-2%) in Lonza starvation medium for 4 h, 24 h or 48 h (n=3-4 donors/group) or undifferentiated S-PBEC cultured on transwells were exposed, after removal of apical medium, to fresh air or WCS from one 3R4F cigarette (University of Kentucky, 2 mg) followed by harvesting of whole-cell lysates after 6 h or 24 h recovery (n=3 donors/group). L-lactate levels **(A)**, PFK 1 enzyme activity **(B)** as well as protein **(C, D)** and mRNA levels **(E)** of HK2 were analyzed in S-PBEC. Representative western blots, including representative parts of the Ponceau S Staining, are shown. Data are presented as mean fold change compared to control (0% CSE or air) ± s.e.m.. Independent donors are represented by open circles, triangles, squares or diamonds. In case of the CSE-exposed S-PBEC experiments, the symbols reflect the mean of technical triplicates. WCS versus air was tested using a two-tailed paired parametric *t*-test. Statistical differences between the various CSE exposure groups (CSE 1% or 2% versus 0% CSE) were tested using an one-way ANOVA (matched/repeated measures) followed by Sidak's post-hoc test for multiple comparisons, and in case of missing values the mixed-effects models was performed. Statistical significance is indicated as $^{\#}p<0.1$ and $^{*}p<0.05$ compared to control (0% CSE or air).

Supplemental tables

Table S1: Human primers sequences used for real-time quantitative PCR analysis.

Gene	Sense primer (5'-3')	Antisense primer (3'-5')
Reference genes		
ATP5B	TCACCCAGGCTGGTTCAGA	AGTGGCCAGGGTAGGCTGAT
B2M	CTGTGCTCGCGCTACTCTCTCTT	TGAGTAAACCTGAATCTTTGGAGTACGC
ACTB	AAGCCACCCCACTTCTCTCTAA	AATGCTATCACCTCCCCTGTGT
PPIA	CATCTGCACTGCCAAGACTGA	TTCATGCCTTCTTTCACTTTGC
RPL13A_1	CCTGGAGGAGAAGAGGAAAGAGA	TTGAGGACCTCTGTGTATTTGTCAA
RPL13A_2	AAGGTGGTGGTCGTACGCTGTG	CGGGAAGGGTTGGTGTTCATCC
Target genes		
BNIP3	AGCGCCCGGGATGCA	CCCGTTCCCATTATTGCTGAA
BNIP3L	CTGCGAGGAAAATGAGCAGTCTCT	GCCCCCCATTTTTCCCATTG
Citrate synthase	GATGTGTCAGATGAGAAGTTACGAGACT	TGGCCATAGCCTGGAACAA
COXII	ACCTGCGACTCCTTGACGTT	GGGGGCTTCAATCGGGAGTA
CYC1	GAGCACGACCATCGAAAACG	CGATATGCCAGCTTCCGACT
DNM1L	CGACTCATTAAATCATATTTTCTCATTGTCAG	TGCATTACTGCCTTTGGCACACT
ESRRA	TGCTGCTCACGCTACCGCTC	TCGAGCATCTCCAAGAACAGC
FIS1	CCTGGTGCGGAGCAAGTACAA	TCCTTGCTCCCTTTGGGCAG
FUNDC1	GAAACGAGCGAACAAAGCAG	GCAAAAAGCCTCCCACAAAT
GABARPL1	ATCGGAAAAAGGAAGGAGAAAAGATC	CAGGCACCCTGGCTTTTGG
HADHA	TGGCTTCCCGCCTTGTC	TGGAGCCGGTCCACTATCTTC
HK2	GTAAATACAGTGGATCTCAATCTTCGGG	CAAGGATTTGAGATGATTCGCTATTCA
KRT8	TCCTCAGGCAGCTATATGAAGAG	GGTTGGCAATATCCTCGTACTGT
MAP1LC3A	CCTGGACAAGACCAAGTTTTTG	GTCTTTCTCCTGCTCGTAGATG
MAP1LC3B	ACCATGCCGTCGGAGAAGAC	TCTCGAATAAGTCGGACATCTTCTACTCT
MFN1	CTGAGGATGATTGTTAGCTCCACG	CAGGCGAGCAAAAGTGGTAGC
MFN2	TGGACCACCAAGGCCAAGGA	TCTCGCTGGCATGCTCCAC
Mt-CytB	ACCCCCTAGGAATCACCTCC	GCCTAGGAGGTCTGGTGAGA
NDUFB3	TCAGATTGCTGTCAGACATGG	TGGTGTCCCTTCTATCTTCCA
NRF1	AGGAACACGGAGTGACCCAA	TATGCTCGGTGTAAGTAGCCA
OPA1	TACCAAAGGCATTTTGTAGATTCTGAGTT	GCATGCGCTGTATACGCCAA
PIGR	CTCTCTGGAGGACCACCGT	CAGCCGTGACATTCCCTG
PINK1	GAAAGCCGCAGCTACCAAGA	AGCACATTTGCGGCTACTCG
PPARGC1A	AAGCCACTACAGACACCGC	TCGTAGCTGTCATACCTGGG
PPARGC1B	GGCGCTTTGAAGTGTTTGGTGA	TGATGAAGCCGTACTTCTCGCCT
PPRC1	GCCCTTTGATCTCTGCTTTGGG	AAGTCTTCCCGGTTGGAGTCAAG
PRKN	GGTTTGCCTTCTGCCGGGAATG	CTTTCATCGACTCTGTAGGCCTG

SDHB	TGGGGCCTGCAGTTCTTATG	ATGGTGTGGCAGCGGTATAG
SOD1	GGTCCTCACTTTAATCCTCTAT	CATCTTTGTCAGCAGTCACATT
SOD2	TGGACAAACCTCAGCCCTAACG	TGATGGCTTCCAGCAACTCCC
SQSTM1	GGTGCACCCCAATGTGATCT	CGCAGACGCTACACAAGTCG
TFAM	GAAAGATTCCAAGAAGCTAAGGGTGATT	TCCAGTTTTCCTTTACAGTCTTCAGCTTTT
TP63	CCACCTGGACGTATTCCACTG	TCGAATCAAATGACTAGGAGGGG

Table S2: Antibodies used for western blotting

Target	RRID	Company	Product number	Dilution factor
Primary Antibodies				
BNIP3	AB_2259284	Cell Signaling Technology	Cat# 3769S	0,736
BNIP3L	AB_2688036	Cell Signaling Technology	Cat# 12396	0,736
DNM1L	AB_10950498	Cell Signaling Technology	Cat# 8570	0,736
ESRRA	AB_1523580	Abcam	Cat# ab76228	0,736
FUNDC1	AB_10609242	Santa Cruz Biotechnology	Cat# sc-133597	0,389
GABARAPL1	AB_2294415	Proteintech Group	Cat# 11010-1-AP	0,736
HK2	AB_2232946	Cell Signaling Technology	Cat# 2867	0,736
MAP1LC3B	AB_915950	Cell Signaling Technology	Cat# 2775	0,736
NRF1	AB_2154534	Abcam	Cat# ab55744	0,736
OXPHOS	AB_2629281	MitoScience LLC	Cat# MS604	0,736
PINK1	AB_10127658	Novus Biologicals	Cat# BC100-494	1,431
PPARGC1A	AB_10697773	Millipore	Cat# 516557	0,736
PRKN	AB_2159920	Cell Signaling Technology	Cat# 4211	0,736
SQSTM1	AB_10624872	Cell Signaling Technology	Cat# 5114	0,736
TFAM	AB_10682431	Millipore	Cat# DR1071	0,736
Secondary Antibodies				
Goat Anti-Mouse IgG Antibody	AB_2827937	Vector Laboratories	Cat#BA-9200	1:10000

Abbreviations:

ATP5B: ATP synthase F1 subunit beta, *B2M*: beta-2 microglobulin, *ACTB*: actin B, *PPIA*: peptidylprolyl isomerase A, *RPL13A*: Ribosomal Protein L13A, *BNIP3*: BCL2 interacting protein 3, *BNIP3L*: BCL2 interacting protein 3-like, *C*itrate synthase, *COXII*: Cytochrome c oxidase subunit II*, CYC1*: cytochrome c-1, *DNM1L*: dynamin 1-like, *ESRRA*: estrogen related receptor, alpha, *FIS1*: fission, mitochondrial 1, *FUNDC1*: FUN14 domain containing 1, *GABARAPL1*: GABA type A receptor associated protein like 1, *HADHA*: hydroxyacyl-CoA dehydrogenase trifunctional multienzyme complex subunit alpha, *HK2*: hexokinase 2, *KRT8*: Keratin 8, *MAP1LC3A*: microtubule-associated protein 1 light chain 3 alpha, *MAP1LC3B*: microtubule-associated protein 1 light chain 3 beta, *MFN1*: mitofusin 1, *MFN2*: mitofusin 2, *Mt-CytB*: Mitochondrial-encoded Cytochrome Beta, *NDUFB3*: NADH:ubiquinone oxidoreductase subunit B3, *NRF1*: nuclear respiratory factor 1, *OPA1*: OPA1, mitochondrial dynamin like GTPase, *PIGR:* Polymeric Immunoglobulin Receptor, *PINK1*: PTEN Induced Kinase 1, *PPARGC1A*: PPARG coactivator 1 alpha, *PPARGC1B*: PPARG coactivator 1 beta, *PPRC1*: PPARG related coactivator 1, *PRKN*: Parkin RBR E3 Ubiquitin Protein Ligase, *SDHB*: succinate dehydrogenase complex iron sulfur subunit B, *SOD1*: superoxide dismutase 1, *SOD2*: superoxide dismutase 2, *SQSTM1*: sequestosome 1, *TFAM*: transcription factor A, mitochondrial, *TP63*: tumor protein 63

BNIP3: BCL2 Interacting Protein 3, BNIP3L: BCL2 Interacting Protein 3-Like, DNM1L: dynamin 1-like, ESRRA: Estrogen Related Receptor, Alpha, FUNDC1: FUN14 Domain Containing 1, GABARAPL1: GABA Type A Receptor Associated Protein Like 1, HK2: Hexokinase 2, MAP1LC3B (or LC3B): Microtubule-Associated Protein 1 Light Chain 3 Beta, NRF1: Nuclear Respiratory Factor 1, OXPHOS: oxidative phosphorylation antibody cocktail (containing NDUFB8: NADH:Ubiquinone Oxidoreductase Subunit B8, SDHB: Succinate Dehydrogenase Complex Iron Sulfur Subunit B, UQCRC2: Ubiquinol-Cytochrome C Reductase Core Protein 2, MT-COI: Mitochondrially Encoded Cytochrome C Oxidase I, ATP5F1A: ATP Synthase F1 Subunit Alpha), PINK1: PTEN Induced Kinase 1, PPARGC1A: PPARG Coactivator 1 Alpha, PRKN: Parkin RBR E3 Ubiquitin Protein Ligase, SQSTM1: Sequestosome 1, TFAM: Transcription factor A, Mitochondrial